Remote sensing and field analysis of the Palaeozoic structural style in NW Libya: The Qarqaf arch a paleo-transfer fault zone between the Ghadamis and Murzuq basins

Jean Chorowicz, Mahmoud Benissa

Remote sensing and field analysis of the Palaeozoic structural style in NW Libya: the Qarqaf arch a paleo-transfer fault zone between the Ghadamis and Murzuq basins

Jean Chorowicz[1*] and Mahmoud Benissa[2]

[1] Sorbonne Universités, UPMC Univ Paris 06, CNRS, Institut des Sciences de la Terre de Paris (iSTeP), 4 place Jussieu 75005 Paris, France corresponding author

[2]Libyan Petroleum Institute, Exploration Department, P.O. Box 6431, Tripoli, Libya, ahmed.mahmoud.benissa@gmail.com

***Corresponding author** jean.chorowicz@upmc.fr

Abstract

The N75°E-trending Qarqaf arch in NW Libya separates the Ghadamis and Murzuq basins. We have updated existing geological maps by remote sensing analysis and fieldwork in order to describe the tectonic style of the Palaeozoic units. We have evidenced a Bir Aishah anticline, a Wadi Ash Shabiyat graben and arrays of sedimentary and/or vein quartz dykes that relate to extension fractures or open faults some of them being filled up by on-going sedimentation. We show that continuous brittle syn-depositional deformation occurred throughout the Palaeozoic and progressively with time focused into major faults. The Qarqaf arch is a Palaeozoic right-lateral fault zone comprising main conjugate dextral N60°E and sinistral N90°E fault families. It also comprises ~N-striking extensional faults with related drag or fault-propagation folds. The Palaeozoic tectonic style is that of rift basins connected by a major transfer fault zone. The arch is as a consequence of strike-slip mechanism. In order to account for distinct folds affecting the Carboniferous strata we argue that partly consolidated silty Devonian and Carboniferous deposits slid in mass by places at the end of

their deposition over tilting Devonian layers. Our model is alternative to the currently considered concept of major Variscan compressional orogen in this area. The regional so called 'Variscan' age disconformity actually is the Triassic early Neo-Tethyan event. These general concepts have potential impact on basin modelling of subsidence, uplift, thermal history and hydrocarbon migration. Any new structural geology study in this area is important for oil exploration.

Keywords

Gargaf; Ghadamis; Libya; Murzuq; Northern Africa; Palaeozoic arch; Qarqaf; remote sensing; tectonics; transfer fault; Variscan belt.

1 Introduction

Arches in sedimentary basins are broad relative linear basement uplifts (Levorsen, 1954), which may be created in compression or extension (Billo, 1985; Laubach and Jackson, 1990). They may form complex anticlinorium structures comprising various oil traps. The N75°E-trending Qarqaf arch in Northwestern Libya between the Ghadamis (north) and Murzuq (south) basins comprises Palaeozoic sedimentary series lying on a Precambrian basement high (Fig. 1) and represents an important oil and gas region. The main (80-90%) source rock is the 'Tanzuft' early Silurian organic-rich shale (Boote et al., 1998; Echikh, 1998). The Palaeozoic structural style is however problematic (Alfestawi, 2001) and this question is generally important for oil exploration (Craig et al., 2008). The arch may be a horst related to extensional tectonics (e.g., Montgomery, 1994) or a major Variscan (Hercynian) compressional structure formed during the late Palaeozoic (e.g., Goudarzi, 1980, Hallet, 2002).

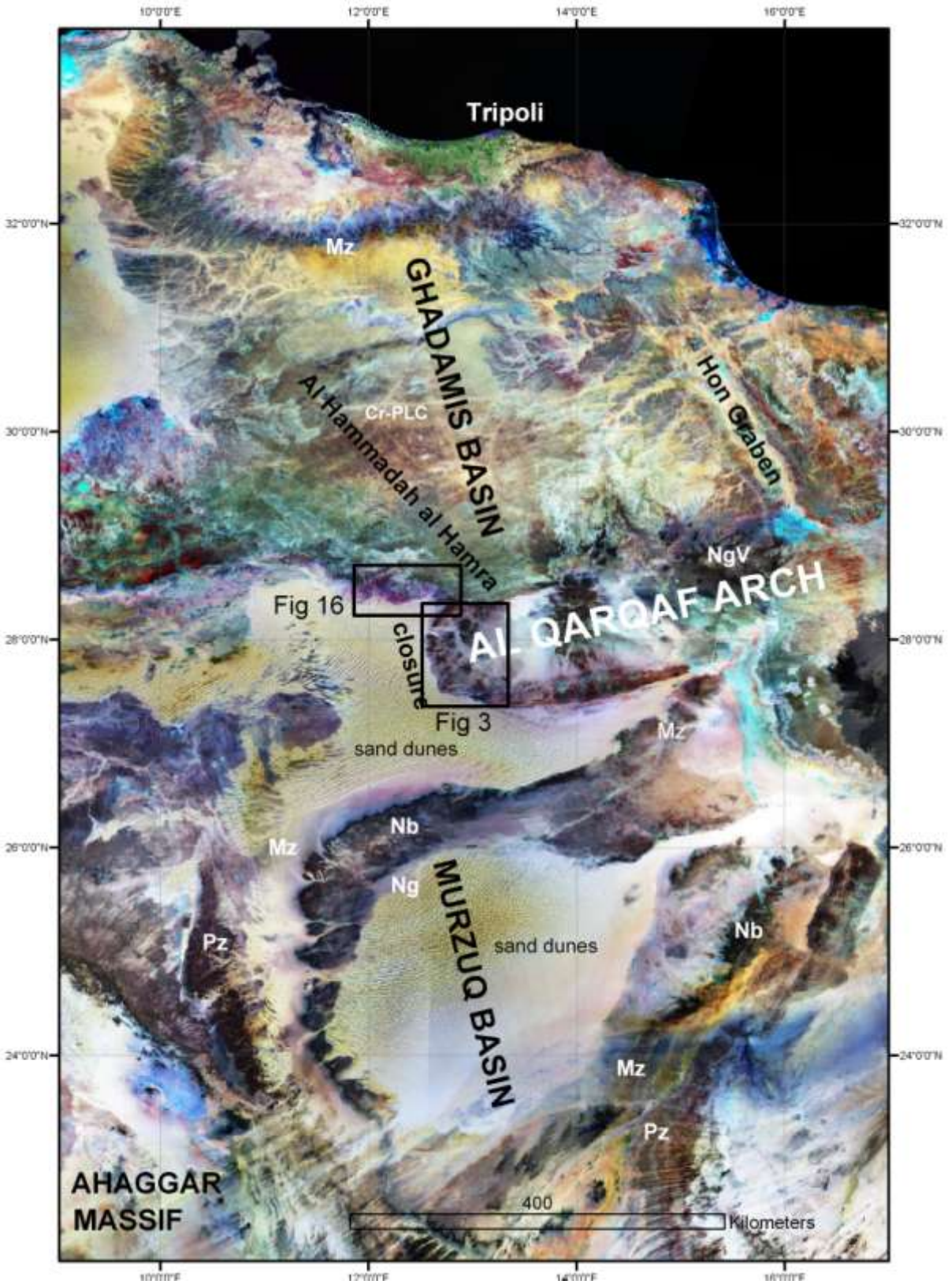

Figure 1. Western Libya illustrated by a mosaic of GeoCover™ Landsat imagery processed by EarthSat. This satellite view is composed of compressed (MrSID format) mosaics of

orthorectified Landsat enhanced Thematic Mapper (ETM+) scenes. It displays a colour composition of three Landsat ETM+ bands, each sharpened with the panchromatic band: • Band 7 (mid-infrared) in red; • Band 4 (near-infrared) in green; • Band 2 (green) in blue. Rectangles: location of study area, divided into two regions: Fig. 3 and Fig. 16. Abbreviations: Cr-PLC: late Cretaceous-Paleocene; Mz: Mesozoic; Nb: Nubian; Ng: Neogene; NgV: Neogene volcanics; Pz: Palaeozoic.

The methodology used in this research is based on remote sensing geological mapping associated with structural analysis in the field, powerful tools for tectonic studies when size, remoteness, and inhospitable area of study induce difficulties of access. Satellite imagery allows locating and precisely mapping outcrops and faults in the frame of a Geographic Information System (Chorowicz and Deroin, 2003; Peña and Abdelsalam, 2006). Global Positioning System (GPS) permitted to carry out field check and structural analysis at locations previously selected by remote sensing.

This paper analyses the Palaeozoic structural style of the Qarqaf arch, focusing on the western closure area (Fig. 1). This leads to clarify and discuss relationships between arch and adjacent basins. In the first section, we review the main geological features of NW Libya. In section 2, we present updated geological maps and a remote sensing study of the fractures, complemented by field fault structural analysis. The discussion section argues that the arch belongs to a Palaeozoic transfer strike-slip fault zone linking adjacent rift basins without intervention of Variscan (Hercynian) regional compression.

2 Main geological features of NW Libya

2.1 Structural units

The 450 km N-S and 370 km E-W Ghadamis basin is disconformably overlapped and largely hidden by late Cretaceous-Paleocene sediments of the Hammadah al Hamra plateau (Fig. 1). The basin comprises up to 4,000 m thick Mesozoic sedimentary series deposited in the southern margin of the Neo-Tethys and resting on a 9,000 m thick comprehensive sedimentary dominantly sandstone Palaeozoic succession (Said, 1974). The Murzuq basin is 700 km N-S and 500 km E-W. Its outlines are shown by early Cretaceous sandstone (Nubian Fm.) overlapping Jurassic and Triassic deposits that in turn almost conformably lie on Palaeozoic sediments. Neogene deposits and a large area of active sand dunes cover its centre.

The Qarqaf arch is a 350 km E-W and 150 km wide anticlinorium lying between the basins. Its northern limb is disconformably overlain by Mesozoic to Paleocene beds. Active sand dunes partly hide the western closure and southern limb. The eastern arch end is intruded and partly overlain by Neogene to recent alkaline volcanics (Bardintzeff et al., 2011; Elshaafi and Gudmundsson, 2016.).

2.2 Lithostratigraphy

The Palaeozoic lithostratigraphic successions in Western Libya have been extensively studied (Desio, 1936, 1960; Burollet, 1960; Banerjee, 1980; Hallett, 2002). They were defined in Algeria, Tunisia and western Al Qarqaf (Bonnefous, 1963; Burollet and Manderscheid, 1967a-b; Conant and Goudarzi, 1967; Massa and Jaeger, 1971; Bishop, 1975; Massa and Moreau-Benoit, 1976; Bellini and Massa, 1980; Klitzsch, 1963, 1966, 1970, 1981; Willis, 1981; Vos, 1981; Whitbread and Kelling, 1982; Massa and Delort, 1984; Castro et al., 1985; Echikh, 1998; Belhaj, 1996, 2000). They are described (Fig. 2) on the basis of five major sedimentary cycles (Karasek, 1981; Rubino and Blanpied, 2000).

Age	Stage	Formation	Symbol in map	Field facies	Thickness	Optical image facies	DEM facies	Radar facies
Carboniferous	Moscovian ..... Bashkirian	**Dembaba**	CuD	carbonate, shale, siltstone, sandstone	100m	blue to black	plateau	
	Serpukhovian	**Assed Jefar**	CuA	carbonate and silty shales	200m	pink purple		
	Visean Tournaisian	**Marar**	CIM	carbonate to silty shale, sandstone and evaporites	800m	dark purple	succession of scarps	bed traces
Devonian	Famennian	**Tahara Dabdab**	DC DuD	sandstone shale shale	150m	dark brown to brown	two ridges	smooth to rough
	Frasnian Givetian Eifelian	**Awaynat** (Aouinet Ouenine)	DmuA	sandstone, silt, carbonate beds	150m	dark pink	flats and ridges	smooth and bed traces
	Emsian	**Bir Al Kasr** (Ouan Kasa)	DmQ	sandstone carbonate		dark brown	massive hills	rough, uniform texture
	Siegenian (Praguian) Gedinnian (Lochkovian)	**Tadrart**	DIT	massive sandstone	40m			
Silurian	Ludlowian Wenlockian Llandoverian	**Tanzuft**	SIT	shales, graptolites	30m	black	depression	rough, uniform
Ordovician	Ashgillian	**Mamuniyat**	OuM	well sorted sandstone, glacial deposits	140m	red-brown	heterog. surface	rough, coarse texture
	Caradocian Llandeilian Llanvirnian	**Melaz Shuqran**	OuS	shale, sandstone, graptolites	60m	blue	flat depression	rough to smooth, contrasted
	Arenigian	**Hawaz** (Haouaz)	OmH	thin grained, massive sandstone	200m	black plateau, brown scarp	massive plateau	rough, fine texture
	Tremadocian	**Late Ash Shabiyat**	OlAu	thin grained sand, shale	250m	light brown	flat depression	grey, irregular
		Early Ash Shabiyat	OlAl	thin grained sandstone	150m	dark rown	homogeneus surface	rough, coarse texture
(late?) Cambrian		**Hasawnah** (Hassaouna)	CH	orthoquartzite, conglomerate, sandy silt	400m	light tone, uniform texture	flat depressions, gentle low hills	light grey, homogeneous texture

Figure 2. Lithostratigraphy of the Western Libya (Bellini and Massa, 1980; Fatmi et al., 1980; Echikh, 1998; Montgomery, 1994; Belhaj, 1996, 2000; Sutcliffe et al., 2000 and Hallett, 2002). The formations are grouped (thick lines) into sedimentary cycles. Thickness of formations is modified from Karasek (1981).

The *first cycle* spans from the Infracambrian-Cambrian to the early Ordovician and starts with a volcanic and detrital Murizidi (Mourizidi) Formation (Fm.), which is not outcropping in the study area, overlain by the **(**late?) Cambrian Hasawnah (Hassaouna, CH) Fm. principally

composed of thin to coarse grained, cross-bedded orthoquartzite and arkose with minor conglomerates, sandy silt and traces of volcanics. The early Ordovician contains tigillite (trace fossil worm tubes emplaced vertically) and comprises: 1) transgressive lower sandstone beds (early Ash Shabiyat Fm., OlAl), 2) middle layers rich in shale (late Ash Shabiyat Fm., OlAu) and 3) upper sandstone beds (Hawaz Fm, OmH). The *second cycle* spans the middle to late Ordovician. Its lower part (Melaz Shuqran Fm., OuS) is varicoloured sandy shale rich in graptolites of Caradocian age (Havlicek and Massa, 1973). Its upper part (Mamuniyat Fm., OuM) consists of tigillite bearing, massive, cross-bedded, medium to fine grained, well sorted sandstone with conglomerate and blocks of glacial origin. The *third cycle* is the graptolite bearing, unconformable transgressive marine late Silurian Tanzuft shale (SIT) and the main source rock for oil in the region. Devonian series form the *fourth cycle* and outcrop in both the northern and southern limbs of Al Qarqaf. The early Devonian (Lochkovian, Praguian) Tadrart Fm. (DiT) is a dark massive, cross-bedded sandstone that outcrops in the northern limb. The middle Devonian Bir Al Kasr Fm. (DmQ) largely outcrops along the southern limb and comprises in its lower part carbonate rocks followed by sandstone and shale. The next middle to late Devonian Awaynat Fm. (DmuA) is conformable and composed of coarse-grained sandstone and layers of shale or carbonate. The Dabdab Fm. (DuD) that follows in the late Devonian is shale. The late Devonian-early Carboniferous Tahara Fm. (DC) that ends this cycle consists of marine-deltaic sandstone and shale. A *fifth cycle* developed during the Carboniferous and started with the Marar (or Mrar, ClM) Fm. made of alternating silty shale, carbonate and sandstone (Lelubre, 1946; De Castro et al., 1985). It is followed upward by the Assed Jefar Fm. (CuA), composed of cross-bedded, ferruginous sandstone, silty shale, beds of shelly carbonate and traces of gypsum. The cycle ends with the Dembaba Fm. (CuD) outcropping in the western part of the Murzuq Basin (Collomb and Heller, 1958/1959). The lower part of the Dembaba Fm. is characterized by grey to white, finely laminated siltstone

and thin-bedded sandstone with limestone and shale. The upper part is mostly composed of dolomite limestone with intercalations of siltstone, marl and claystone. The formation is dated Bashkirian to early Moscovian (Banerjee, 1980).

2.3 Tectonics

Many of the basement tectonic trends of North Africa were set during the Panafrican event (Kröner, 1991; Echikh, 1992, 1998; Boote et al., 1998) and this includes the Qarqaf arch for it is part of the major Oued Amded lineament connected to the Ahaggar Massif (Dautria and Lesquer, 1989). Several authors (Goudarzi, 1980; Ziegler, 1988; Scotese and McKerrow 1990; Kröner, 1991; Echikh,1992, 1998; Boote et al., 1998; Scotese et al., 1999; Al Fastawi, 2001; Hallett, 2002) consider Libya to have been affected during the Palaeozoic by two major tectonic events: 1) the Caledonian orogeny due to the collision of Laurentia (North America) with Africa in the late Silurian-early Devonian, forming broad NW-trending uplifts and troughs; 2) the Variscan orogeny due to the collision of Gondwana with Laurasia forming the super-continent of Pangea in the late Carboniferous-Permian, responsible for ~E-W structures.

The Palaeozoic structural style in Al Qarqaf however remains unclear. The arch structure was first described to have been a basement uplift bounded by ~N75°E-striking high angle faults during the Ordovician, Silurian and Devonian (e.g., Klitzsch, 1970; Hammuda, 1980). Normal and strike-slip faults are mentioned. The Caledonian event is evident for Said and Kanes (1985) but they stated that the structures of the adjacent Ghadamis and Murzuq basins give preference to a model of rift tectonics and basins subsidence, followed by compression landward of the orogen during the Variscan orogeny. The arch was for Montgomery (1994) created by compression at the end of the Panafrican orogeny and the faults were rejuvenated in extension during the late Silurian-early Devonian Caledonian orogeny. Most authors agree that late extensional reactivations are related to the early Mesozoic (early to mid-Triassic)

Neo-Tethyan continental rifting. Guiraud and Bosworth (1997), Guiraud (1998) and Guiraud et al. (2005) have shown reactivations in northern Africa related to Cretaceous-early Cenozoic rifting with short compressive episodes in the southern Neo-Tethys.

3 Structural geology study

3.1 Mapping the lithostratigraphy

3.1.1 Methodology

We first updated existing geological maps using a remote sensing and GIS approach (Chorowicz and Deroin, 2003). One of the main concerns was to provide clues for identification of faults from displacements. The study area is covered by geologic maps of Libya at 1:250,000 (Gebel Qararat-al-Marar, 1983 and Gebel Idri, 1984) and by the Geological Map of Libya at 1:1,000,000 (1985). We principally analysed multispectral Landsat ETM+ imagery at 30 and 15 m ground pixels. We also made use of images at 30 m ground pixel acquired by ERS SAR (European Remote Sensing Satellite Synthetic Aperture Radar) operating in the C band and of 90 m ground pixel shadowed DEM (Digital Elevation Model) images produced from radar interferometry of the Shuttle Radar Topographic Mission (SRTM). Each lithostratigraphic unit in this multisource imagery displays typical image facies, e.g., colour, morphology, roughness, texture, which complement the more classical field facies (Fig. 2).

Mapping was carried out in the frame of the Geographic Information System ArcGIS used for georeference or geocode all the remote sensing data and existing geological maps in a common projection system (GCS-WGS-84). The radar images were not corrected for geometric distortions that normally occur in high relief due to radar acquisition geometry. The study area however has large flat surfaces that render such processing not fully necessary. We also mapped the road and trail system for finding the best ways to reach faults in the field.

Comparing the updated geological map (Fig. 3B) and the previous ones (Fig. 3A) provides new evidences that are keys to understand the structural style of the arch. Our map is somewhat simplified and displays fewer small outcrops than the original 1:250,000 maps, e.g., many small patches of the early Devonian in the south are not shown. This is because the scale of mapping in our imagery – typically at 1:100,000 – is less precise than mapping in the field with the help of aerial photographs – typically at 1:30,000. Most small outcrops also don't have a geomorphic expression sufficiently developed to be identified. These details were not critical to our investigation and they can be analysed in the older maps.

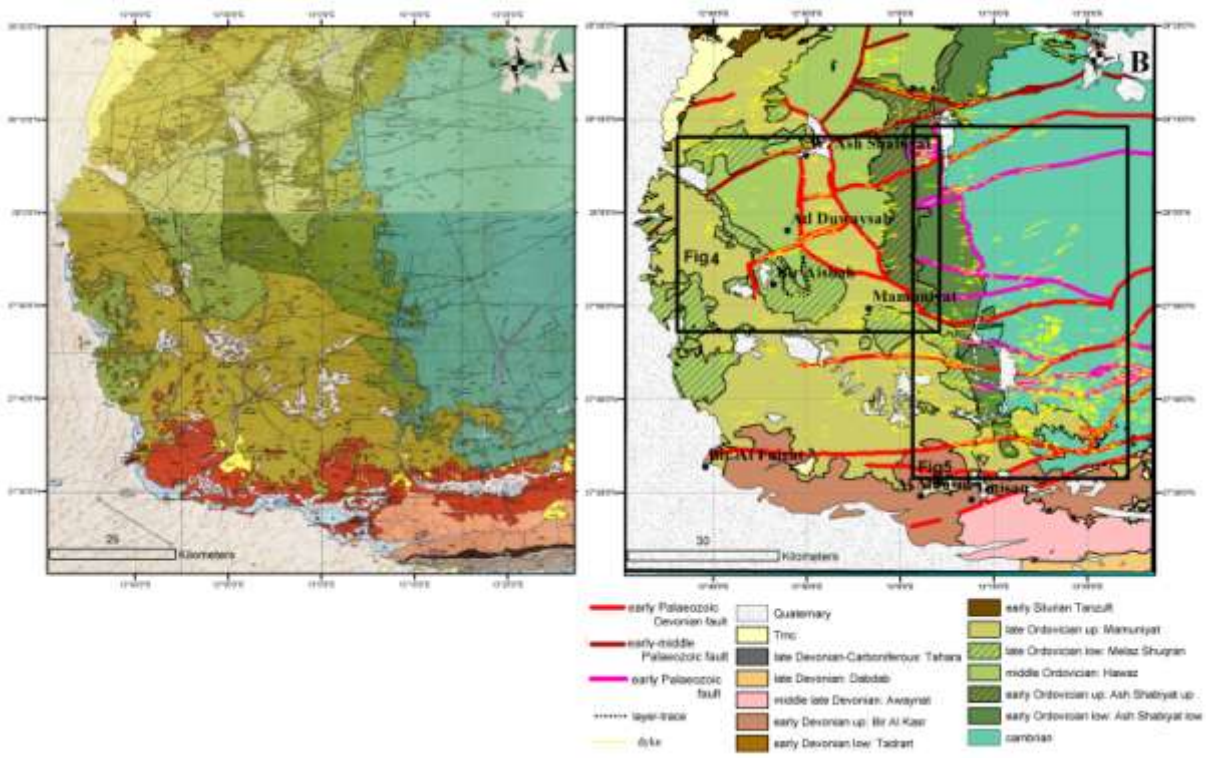

Figure 3. Updated geological map (B) compared to the 1:250,000 geological map of Libya (A) that comprises from north to south extracts of the sheets Gebel Qararat-al-Marar (1983) and Gebel Idri (1984). Rectangles in map B are frames of Figure 4 (left) and Figure 5 (right).

3.1.2 Main results of mapping

A salient result is the evidencing of the Bir Aishah anticline, axis trending N160°E (Fig. 3B). We drew traces of bedding from Landsat ETM+ and ERS SAR images (Fig. 4A, B and C) in what we recognized in the field from interbedded shale and fine grained sandstone to be the Melaz Shuqran unit (late Ordovician, OuS). This outcrop was not shown in the pre-existing map (Fig. 4E) but mentioned by Blanpied et al. (2000). Measurements in the field (red numbers and associate symbol in Fig. 4B) show that dips are divergent. The anticline core consists of massive outcrops of Hawaz sandstone (middle Ordovician, OmH) bordered by a semi-circular low area - in map view - of late Ordovician Melaz Shuqran rocks shaping a typical anticline closure in both the older map and ours. The Mamuniyat unit (late Ordovician, OuMe) has the morphology of a cuesta (Fig. 4F) with dip-slope surfaces characterized by light tones in the Landsat image (Fig. 4A) and light grey tones in the radar image (Fig. 4C). The geologic cross-section XY (Fig. 4) we have drawn from the map shows that the Bir Aishah anticline is gentle.

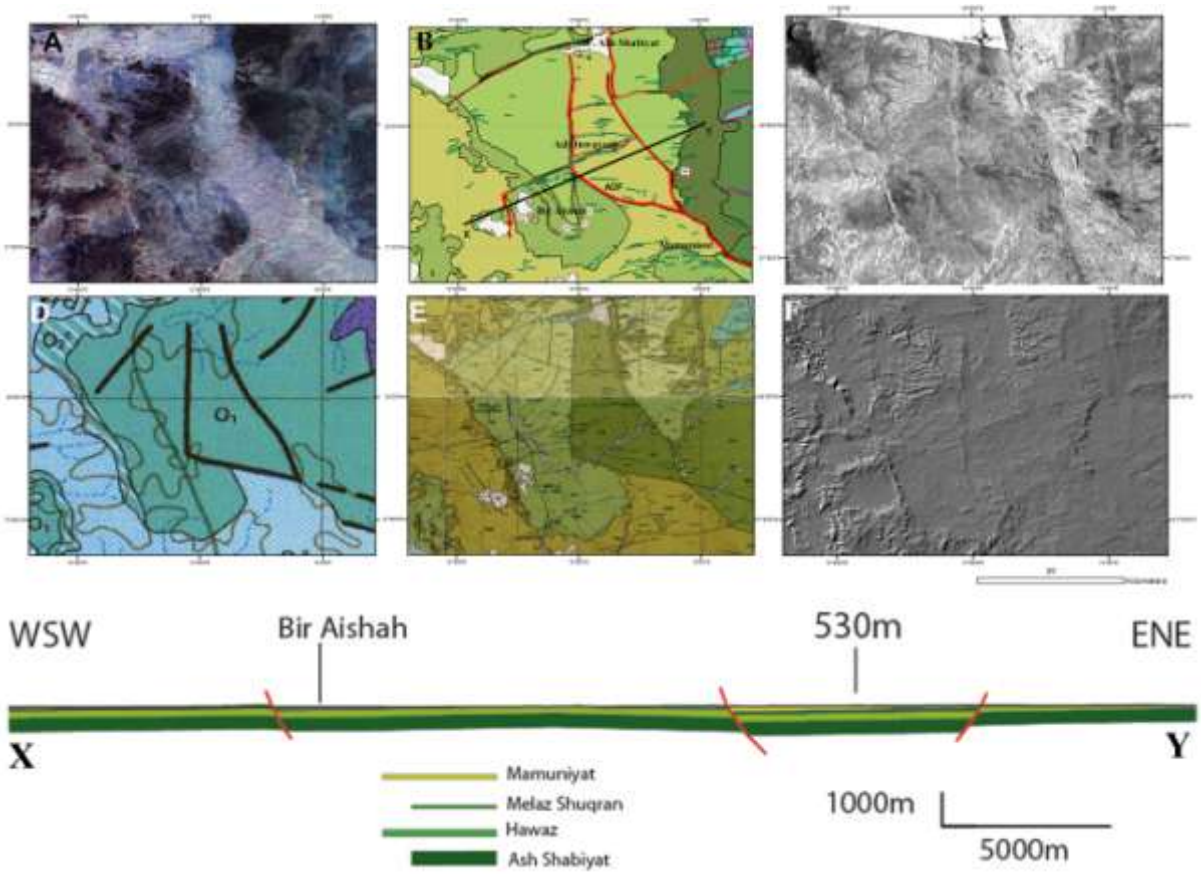

Figure 4. Area of Bir Aishah; see location in Figure 3B. A: Landsat ETM+ image (blue, band 1; green, band 3; red, band 5). B: new geological map; same legend as Figure 3. C: ERS SAR image. D: extract of the Geological Map of Libya at 1:1,000,000 (1985). E: extracts of the geologic maps of Libya at 1:250,000 of Gebel Qararat-al-Marar (1983) and Gebel Idri (1984). F: shadowed SRTM DEM image; false illumination from NW. XY: geologic cross-section along the WSW-ENE line in B; no vertical exaggeration.

Another result concerns the fault bounded Wadi Ash Shabiyat block (Fig. 3B). N70°E-striking fault zones cut this roughly N-S outcrop in the middle. The northern, eastern and western border faults are evident in the Landsat image (Fig. 4A). The southern N120°-striking border fault (ADF in Fig. 4B) is already drawn on existing maps but not well expressed in the images for it forms a faint line but we mapped it in the field. The outcrops of this block are

attributed to the late Ash Shabiyat Fm. (OlA or OlAu) of early Ordovician age in existing 1:250,000 geological maps (Fig. 4E). The same outcrops are noted O_1 (lower-middle Ordovician) in the geological map of Libya at 1:1,000,000 (Fig. 4D). They however are very similar in the imagery to those of the late Ordovician Mamuniyat Fm. for they express the same surface characteristics as that forming the type-locality area at Mamuniyat (Fig. 4B) south of the ADF line. These type-locality surfaces are light-pink purple in the Landsat image (Fig. 4A) and light-grey with a unique heterogeneous texture in the radar image (Fig. 4C). The Landsat image expression north of the ADF line is exactly the same as at Mamuniyat and in the radar images almost the same. Image facies in the entire block is everywhere the same and similar to that of the type-locality. Surfaces corresponding to the late Ash Shabiyat Fm. on both western and eastern sides of the block are much darker in the Landsat image (lower albedo) than others. We deduce that the whole surface of the Wadi Ash Shabiyat block consists of Mamuniyat sandstone. Determining the age of these rocks in the field is difficult because all are sandstones with important variations in outcrop local aspects due to syn-depositional glacial episodes. Blanpied et al. (2000) explain that precise dating of the Mamuniyat sandstone in the Qarqaf area would require light drilling equipment for in situ recovery of non-weathered micro faunas (chitinozoans and conodonts) or for palynological analysis (El-Mehdawi, 2000).

3.2 Tectonics

3.2.1 Approach

Our method to study the deformation style at regional scale (e.g., Fig. 5) first consisted in mapping tectonic patterns from satellite imagery. We afterward accomplished fieldwork in order to assess actual mechanisms of most faults by structural analysis at key sites. We assumed that regional scale fault deformation principally includes movements along the major faults, i.e., the fault arrays that can be observed, identified and mapped from remote sensing

(Chorowicz et al., 2004). Smaller faults or other fractures also participate to regional deformation or may just express local strain or burial history and may permit to carry out structural diagenesis analysis (Laubach et al., 2010) but need to be observed in the field, samples or drill cores, necessitating much more ground survey and structural analysis sites, which we could not perform in our remote desert study area. We identified three types of tectonic lines: dykes, faults and joints.

We also analysed the fracture system for age purpose (e.g., Fig. 5). The lithology of the numerous sedimentary dykes, once open fractures, permitted to deduce ages from infill facies. Faults that are unconformably covered by sediments can be dated and we also used information from crossing and abutting relations. We choose not to carry out a satellite lineament analysis similar to that done from a multisource dataset by Al Fasatwi et al. (2003). This would have been possible from the various imagery we have but we preferred to map only obvious fractures because lineaments are uneasy to define and generally subjected to controversy (Chorowicz, 1980).

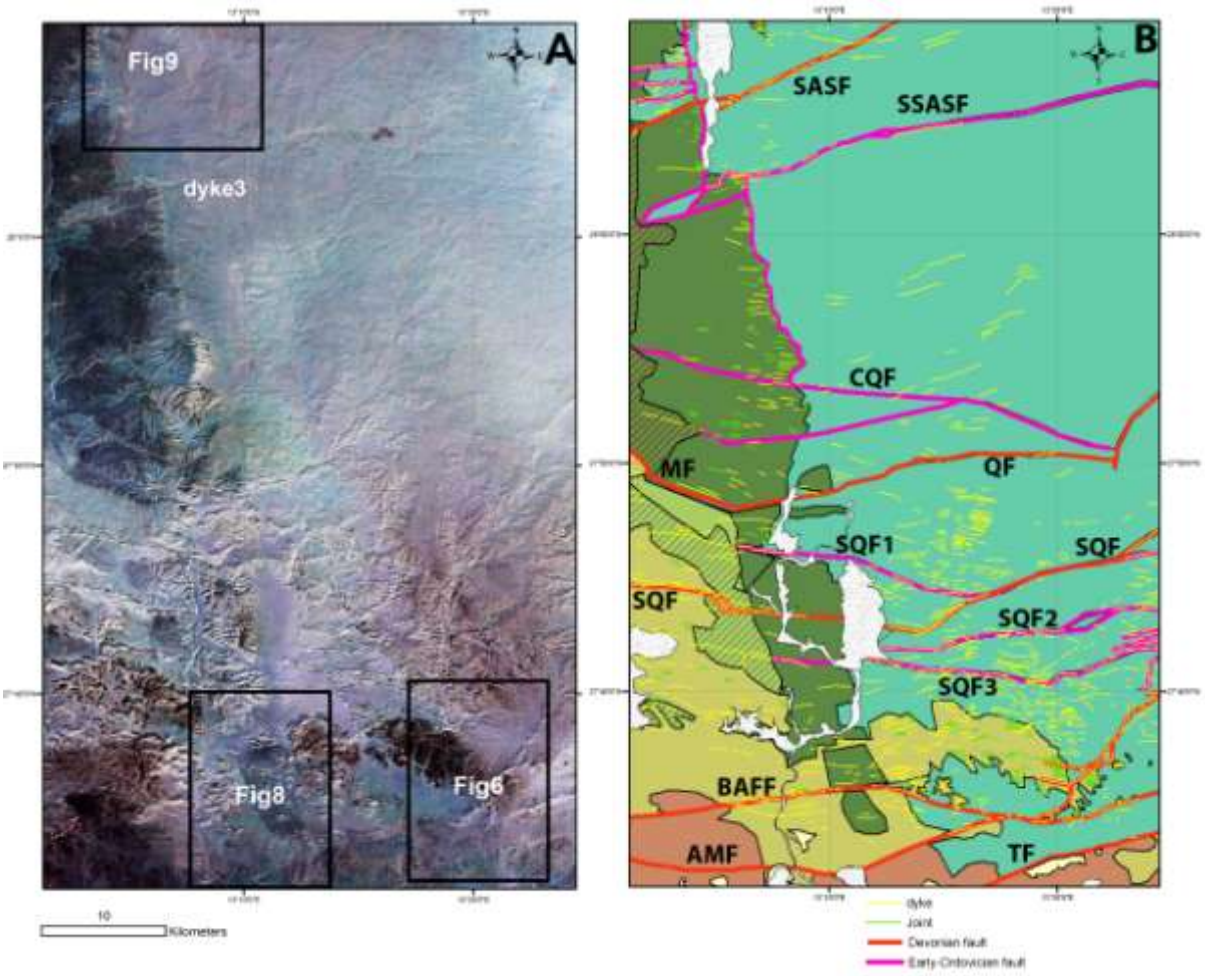

Figure 5. Fracture mapping of the southern part of Al Qarqaf (location in Figure 3B). A: colour composite Landsat ETM+ image (blue, band 1; green, band 3; red, band 5). B: mapping including faults and sedimentary and/or vein quartz dykes. Lithostratigraphy: see legend of Figure 3. Rectangles: location of Figs. 6, 8 and 9. AMF, Al Mansur fault. BAFF, Bir Al Furat fault. CQF, Central Qarqaf fault. MF, Mamuniyat fault. F1F, F1 fault. QF, Qarqaf fault. SASF, South Ash Shabiyat fault. SQF, South Qarqaf fault. SQF1, South Qarqaf fault 1. SQF2, South Qarqaf fault 2. SQF3, South Qarqaf fault 3. SSASF, South-South Ash Shabiyat fault. TF, Tmisan fault. See also the pull-apart relay zones that indicate strike-slip motion, right-lateral pa1 along SQF, left-lateral pa2 along SQF2 and right-lateral pa3 along SSASF.

3.2.2 Fracture mapping

Dykes form sub-vertical wall-like objects with a light tone along the illuminated slope. Illumination is from the south in optical images, the west in our ERS SAR images and we choose false illumination from the NW in the shadowed DEM image. The other side – back to illumination - is an adjacent dark line (Fig. 6A: see for instance at location ‘dyke’). All the dykes we found and discussed are sedimentary and/or vein quartz in composition and not igneous. We propose to sort the dykes according to their length.

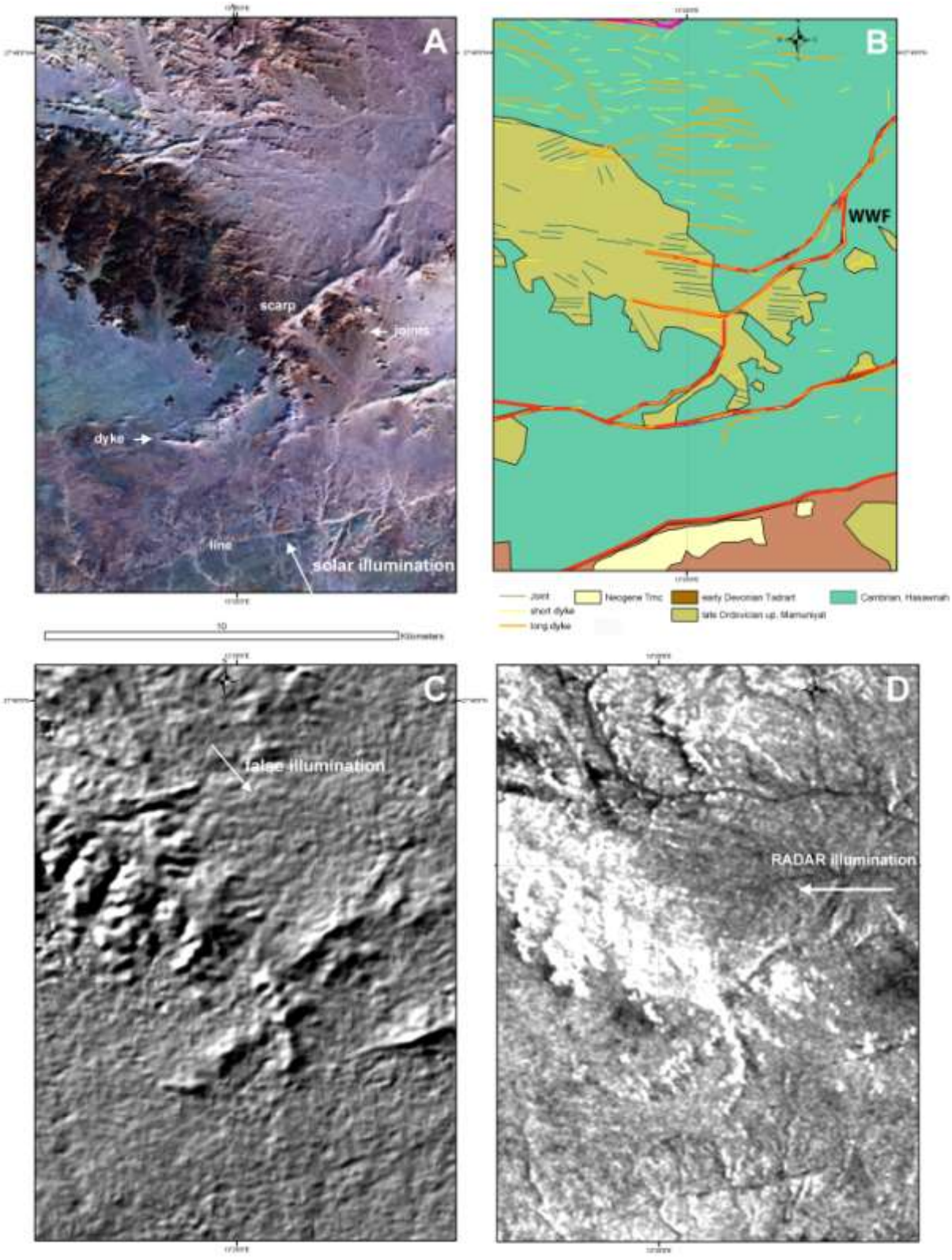

Figure 6. Examples of dyke and fault interpretation from different image types. A: colour composite Landsat ETM+ image (blue, band 1; green, band 3; red, band 5). Sun illumination is from SSE. B: multisource mapping, including dykes and joints, see legend of Figure 3. C:

shadowed DEM image; we choose false illumination from the NW. D: SAR ERS image, radar illumination from the east. Comparison of A and D also shows how Mamuniyat sandstones, which are brown in the Landsat image but white in the SAR ERS image because of roughness, are different from the Asawnah sandstone. Location in Figure 5A. WWF, Wade Wenzrek Fault.

Short dykes have sharp ends but some are too small to be mapped in satellite imagery (Fig. 7A). Those that we observed from space have lengths from ~ 0.1 to 0.6 kilometres and widths > 1 m. They don't significantly displace the rock boundaries or layer traces they cross and form families of parallel lines (e.g., Figs. 5 and 6). Some are S- or Z-shaped (Fig. 8). They may form en-echelon aligned clusters over distances of several kilometres (Fig. 9). All these characteristics relate the short dykes to extension fractures (Gudmundsson, 1992). They opened once and were filled up with rocks that now are less weathered-eroded than the nearby layers.

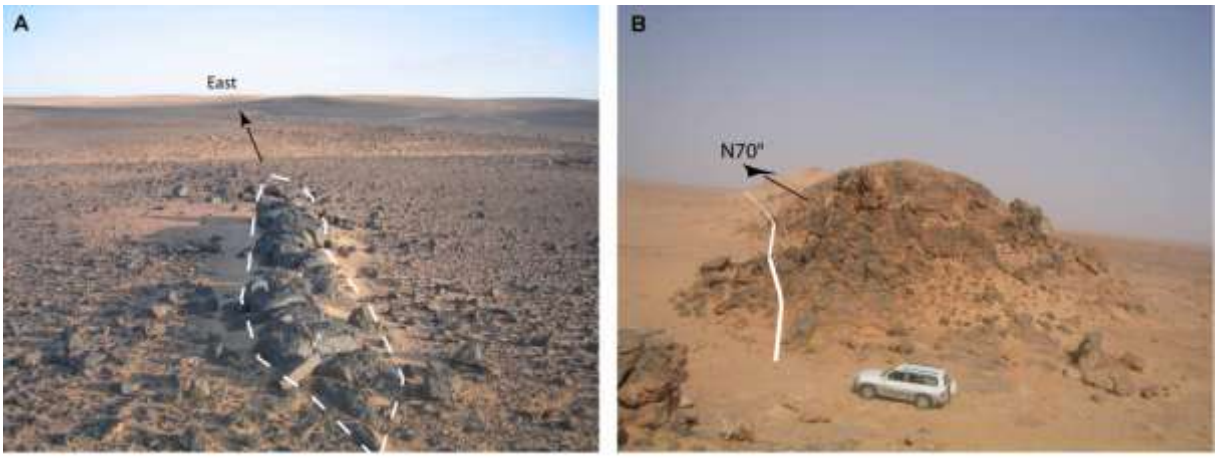

Figure 7. Dykes in the field. A: short sedimentary dyke of dark grey orthoquartzite, too small to be observed in our imagery. B: long sedimentary dyke composed of monogenic breccias and sandstone, part of a large fault at location ‘dyke3’ in Fig. 5A.

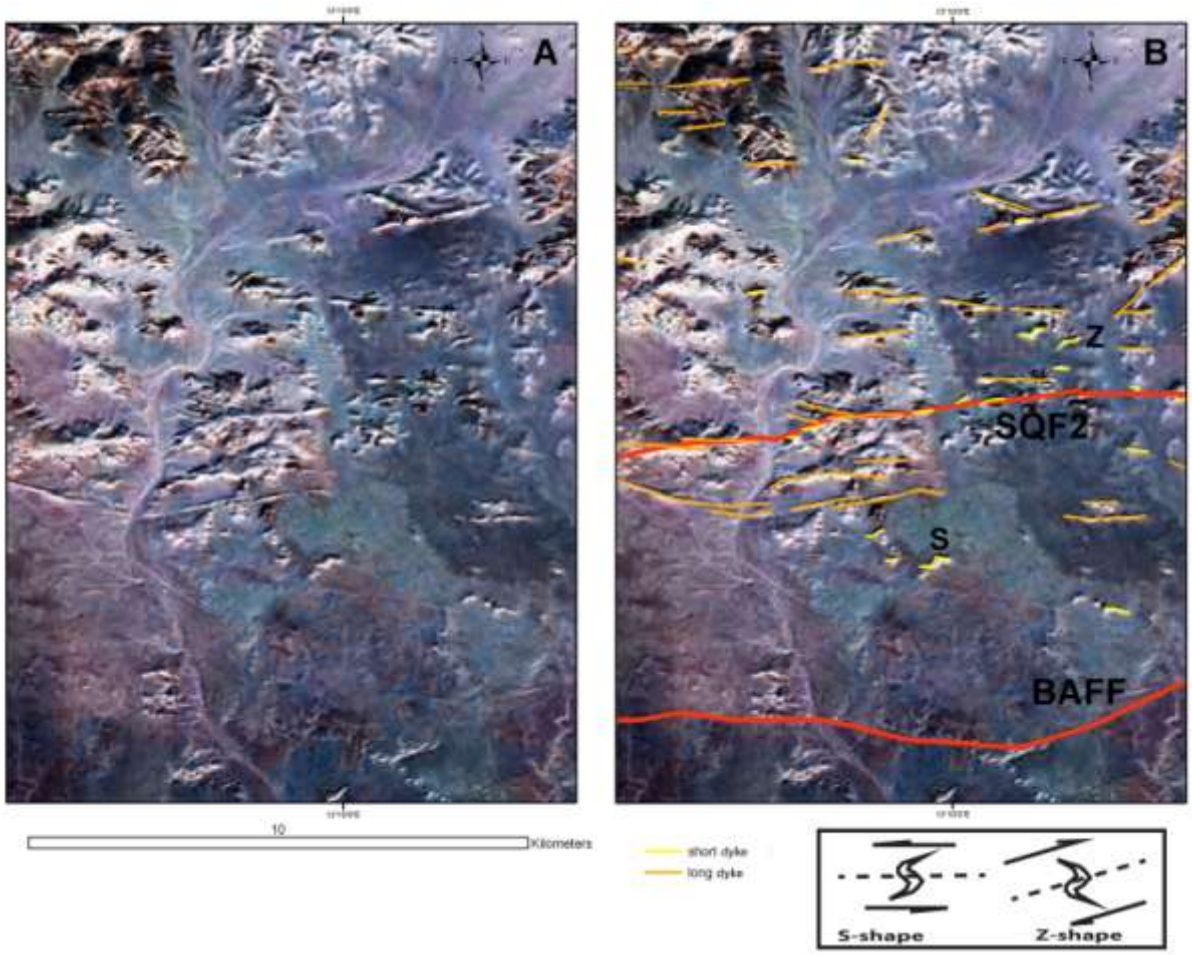

Figure 8. Families of dykes with clear examples of S- and Z-shaped short dykes. A: colour composite Landsat ETM+ image (blue, band 1; green, band 3; red, band 5). B: map of dykes and faults. Location in Figure 5A. Red lines are Devonian faults, BAFF (Bir Al Furat fault), SQF2 (South Qarqaf fault 2). Legend insert: scheme of S- and Z-shaped extension fractures along ductile faults (dots) and related sense of movement, from Moores and Twiss (1992).

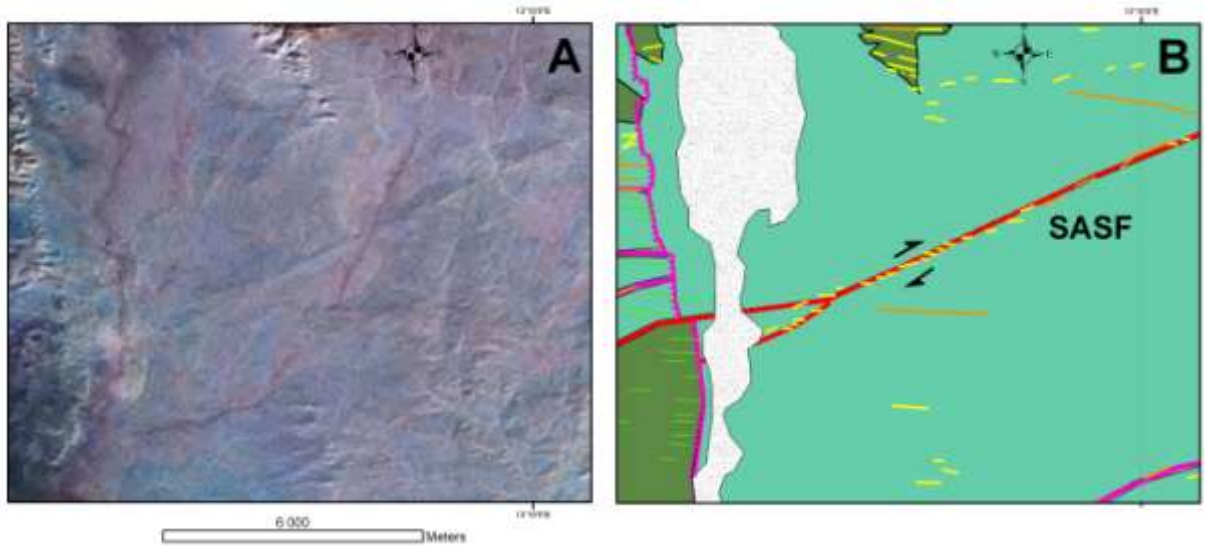

Figure 9. En-echelon succession of short dykes along a fault (SASF, South Ash Shabiyat fault). Location in Figure 5A. Succession is equivalent to a ductile fault (Ramsay, 1987), which changes ENE-ward into a brittle fault. This fault has a dextral strike-slip component shown by right-stepping en-echelon extension fractures. A: colour composite Landsat ETM+ image (blue, band 1; green, band 3; red, band 5). B: mapping, same legend as Fig. 3, early Ordovician faults in purple (F1F, F1 fault), the SASF Devonian fault in red.

Long sedimentary dykes are several kilometres in length (Fig. 5). Width in the field is typically 2 to 100 m (Fig. 7B). They may belong to successions of aligned shorter dykes.

Sub vertical faults in the images form lines several tens of kilometres in length or are made of aligned long dykes successions or long arrangements of shorter dykes (Fig. 6). En-echelon families of extension fractures forming alignments (e.g., Fig. 9) are indicative of crack or fault propagation (Pollard et al., 1982; Ramsay, 1987). Faults may also be revealed: 1) by the morphology of narrow linear depressions that are a consequence of easier weathering and erosion along mylonitic rocks of fault plane; 2) scarps due to difference in lithology on opposite fault sides (e.g., Fig. 6A, ‘line’ and ‘scarp’). Faults are confirmed by offsets: horizontal throw components can be observed in satellite imagery by displaced objects such

as rock boundaries, bed traces, other faults or extension fractures (Fig. 5). Faults may bring rock units into abnormal contact. Some faults (e.g., Fig. 5) are undoubtedly of the strike-slip type because they include rhomb-shaped relay zones of pull-apart geometry (Burchfiel and Stewart, 1966).

Joints form thin, short straight lines with a light tone along the illuminated slope while the other side is an adjacent dark line closer to illumination (Fig. 6, 'joints'). They are characterized by easier gully erosion and constitute families of parallel lines (Fig. 6). These lines are hardly visible in the Landsat images and appear in some places such as near a cuesta. It was not possible to get there on the ground to find out what they really are. They may be small fractures that show neither significant relative movement nor opening filled by dyke at the scale of imagery, quite similar to joints at outcrop scale (Engelder, 1993), which can be remote sensed through local easier erosion. They may be sedimentary dykes which infill is softer than the nearby beds. They may alternatively have formed by local decompression along a cuesta recently shaped by erosion. .

3.2.3 Main results of fracture mapping

The fracture set in our updated geological map (Fig. 10) is significantly different from that of the Geological Map of Libya at 1:250,000 (Fig. 3A). Comparing maps is however not our objective. We have drawn on the one hand fewer fault lines for many do not appear in our imagery because resolution is limited to 15 m. We obtained on the other hand a different trace for some major faults and we extended several of them. Our benefit is the sorting of the fracture system into: 1) short dykes, related to extension fractures; 2) long dykes interpreted to be minor faults; 3) major faults; 4) local joints. We choose not to draw all the long dykes systematically as faults but we think they are minor faults for most part, i.e., with no displacement observed from the space imagery we used. The major fault families strike N60°E (N55°E to N65°E) and N90°E (N80°E to N110°E). A N165°E-striking family also is

distinctive. Most short dykes strike N70°E to 100°E, mean at N85°E. We checked this mapping in the sites where we performed structural analysis and by landscape analysis along our field surveys.

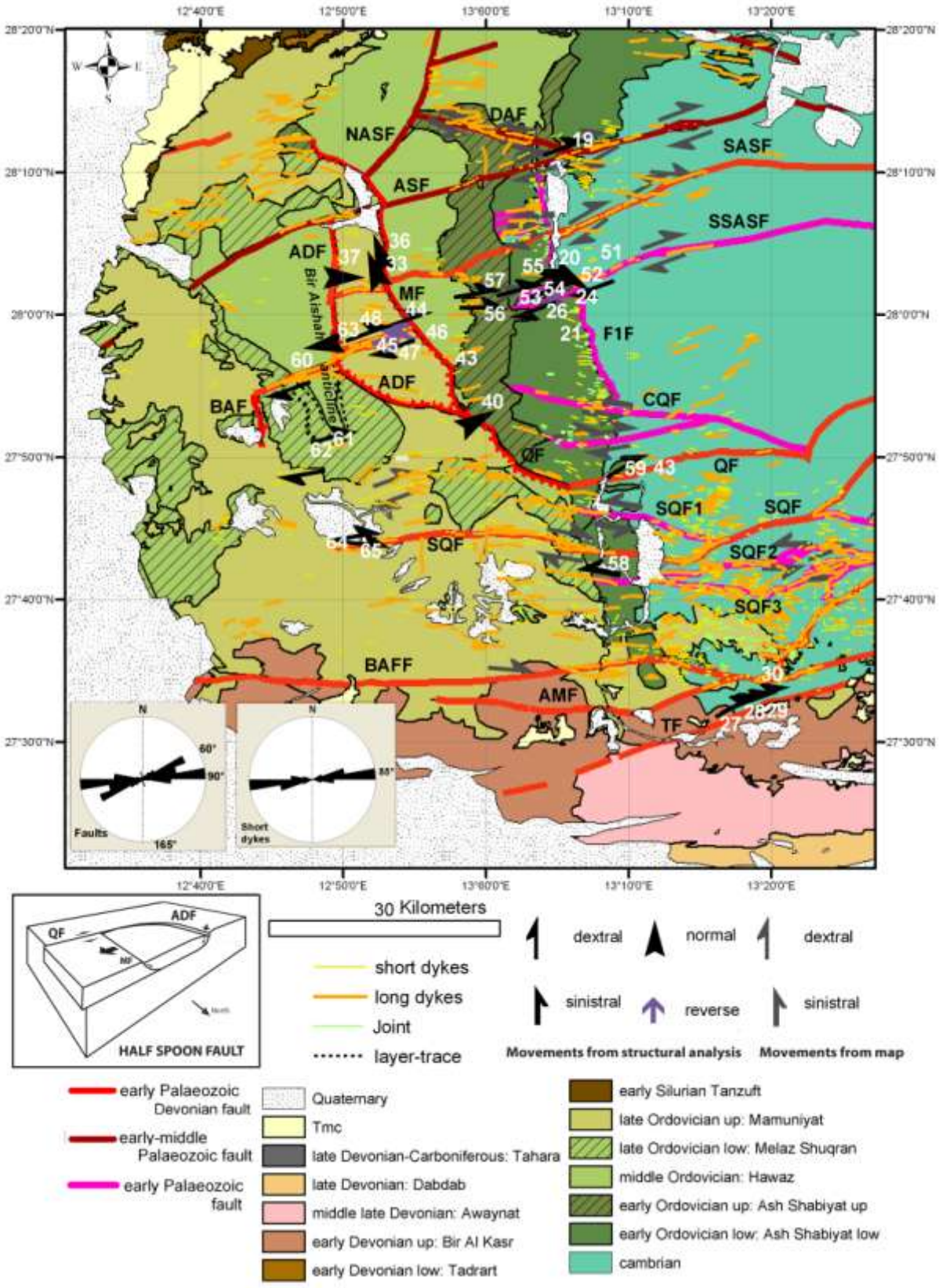

Figure 10. Map of fractures in western Al Qarqaf from remote sensing analysis and compilation of previous maps. Indications of movements are deduced from local map patterns

(arrows in grey) or structural analysis (arrows in black, site numbers in white, copied from Figs. 13 and 14). Inserts in left-bottom corner: rose diagrams in cumulate lengths of fault strikes (two main families at N60°E and N90°E, and a minor family at N165°E) and short dyke strikes (N85°E)**.** Insert in legend: block diagram of a half spoon fault, view from NE. ADF, Al Duwanah fault. AMF, Al Mansur fault. ASF, Ash Shabiyat fault. BAF, Bir Aishah fault. BAFF, Bir Al Furat fault. CQF, Central Qarqaf fault. DAF, Djebal Awaz fault. F1F, F1 fault. MF, Mamuniyat fault. NASF, North Ash Shabiyat fault. QF, Qarqaf fault. SASF, South Ash Shabiyat fault. SQF, South Qarqaf fault. SQF1, South Qarqaf fault 1. SQF2, South Qarqaf fault 2. SQF3, South Qarqaf fault 3. SSASF, South-South Ash Shabiyat fault. TF, Tmisan fault. WWF, Wade Wenzrek fault.

3.2.3.1 Ages of fractures

Ages of sedimentary dykes are deduced from their lithology observed in the field. *Short dykes* are former extension fractures filled by dark grey homogeneous fine grained orthoquartzite without gouge quartz crystallization or figures showing injection (Figs. 7A, 8 and 9). Opening and sedimentation are almost coeval. Lithology of fills and host layers are generally similar. This implies that the diagenesis and compaction of sediment mass was strong enough to be prone to brittle deformation when extension fractures formed (Laubach et al., 2009). *Long dykes* are of two main rock types: 1) sandstone, orthoquartzite and breccias sometimes cut by striated 1 cm- to 10 cm- thick white quartz veins; 2) up to 20 cm-thick complex networks of striated white quartz veins. We interpret: - type 1 corresponds to large open extension fractures or to open faults filled by on-going sedimentation and eventually cut by synkinematic quartz crystallization occurring later in depth during continuing tectonic activity under greater charge; - type 2 has recorded several periods of tectonic activity and quartz crystallization under greater pressure in depth. When brittle extensional deformation affects

sands submitted to early cementation, fractures tend to open, i.e. walls tend to move apart from each other and the gap may be filled by quartz growth. But if opening rates exceed the fastest rate of crystal growth, fractures remain open (Gale et al., 2010) and trap sediments from the surface or breccias from walls falling-in. In other configurations (site 19, Fig. 11) strike-slip motion may produce pull-apart shaped openings filled by sedimentary breccias. Fills in such sedimentary dykes experienced the same transformations than host layers with however perhaps more recrystallization leading to orthoquartzite in reason of easy liquid percolation through rapidly opening features, followed by long time hydraulic activity expected in deep basins (Becker et al., 2010). Sedimentary dykes are widespread in the Cambrian to late Ordovician sandstones, especially along and near fault arrays (Fig. 10). They might be related to the formation of regional scale structures (Olson et al., 2009). White quartz fault dykes are frequent in the Cambrian but their proportion is less in the Ordovician.

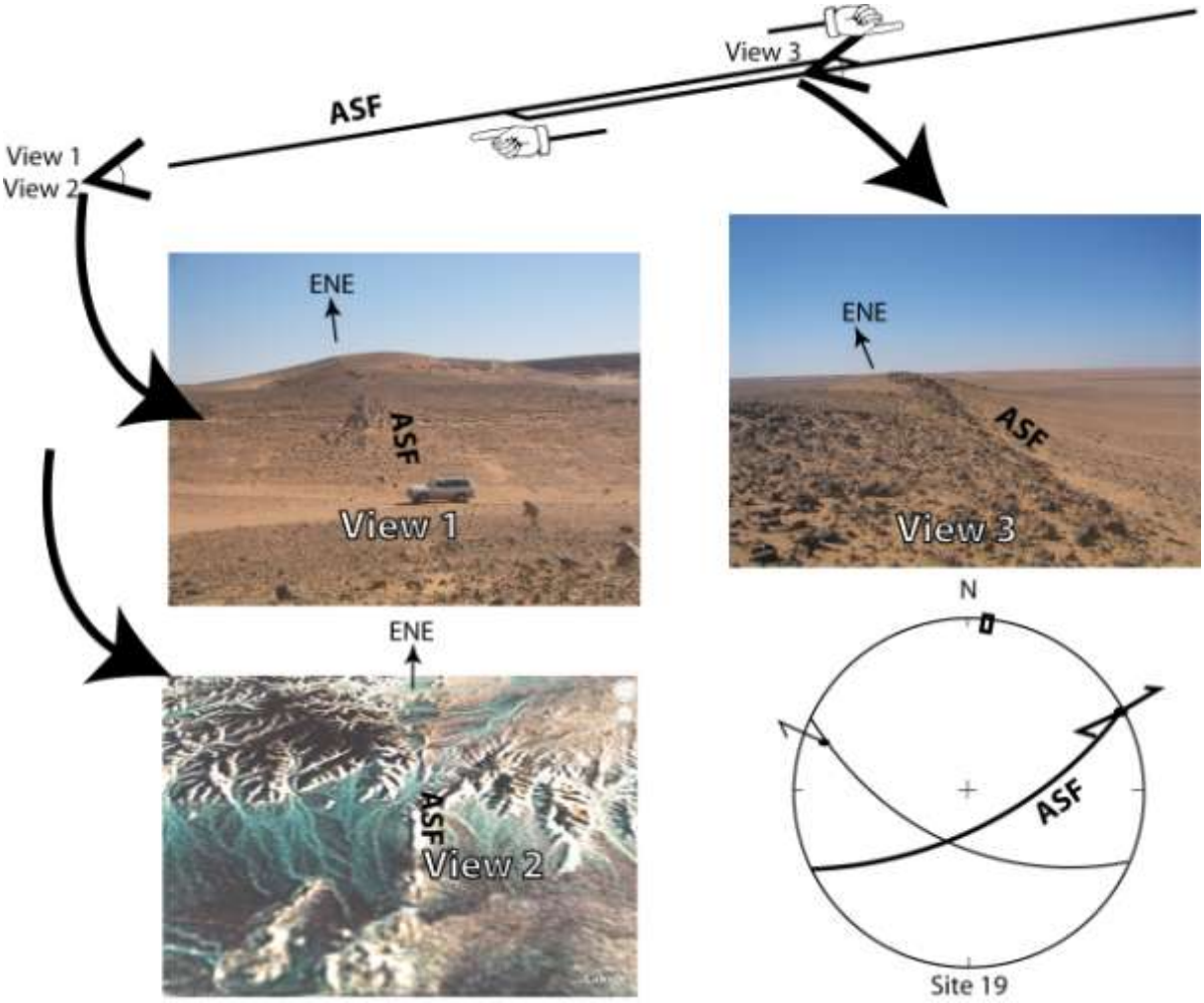

Figure 11. Long dyke along the Ash Shabiyat fault (ASF). All views are to ENE (see image orientation in view 2 and points-of-view in map sketch on top of figure). View 1: in the field. View 2: from Google oblique space imagery. View 3: in the field, showing the sharp ENE end of the pull-apart feature. Site 19: plot of structural measurements at site 19 (location in Fig. 10, along ASF). Schmidt projection, lower hemisphere. Symbol explanations are in legend of Fig. 13. Field measurement confirms ASF is dextral.

Fault ages can partly be deduced from the lithology of the long dykes that lie along or near their trace: sedimentary dykes, white quartz dykes or sedimentary dykes cut by white quartz veins. The ~N-striking F1F and almost all the ~E-W faults affect the Cambrian and consequently postdate the late Precambrian major Panafrican compressive event (Fig. 10).

Last time of activity is known for individual faults when they are unconformably overlain, or according to relative timing from crossing and abutting relationship and orientation. Three categories can be distinguished. 1) Early Palaeozoic (Cambrian to early Tremadocian) faults such as SSASF, CQF, SQF1, SQF2 and SQF3 are unconformably overlain by late Ash Shabiyat (early Ordovician) layers (Figs. 10 and 5). 2) Early to middle Palaeozoic faults such as ASF are underlined by sedimentary long dykes in the Cambrian Hasawnah Fm. that attest they began during the Cambrian but ended before sedimentation of the unconformable latest Ordovician (Mamuniyat Fm.). They are reworked by white quartz veins. DAF may be coeval for it is associated with long dykes in the late Ash Shabiyat formation and abuts against ASF. 3) Early Palaeozoic to late Devonian faults such as BAFF, AMF and TF were still active in the late Devonian for they clearly cut middle Devonian units in the southern arch rim. Several authors (e.g., Conant and Goudarzi, 1967; Hammuda, 1980; Karasek, 1981; Hallett, 2002) wrote that the main faults affecting Al Qarqaf are late Devonian in age. We agree with this opinion as for their latest activity.

The N-striking ADF and MF progressively change in strike SE-ward and merge to form the SE-striking QF, which turns to ENE-strike and is associated with long sedimentary Cambrian-Ordovician dykes that attest it had some activity at this time. These faults and associate long dykes cut the late Ordovician Mamuniyat Fm.; they consequently were still active in the late Devonian. SASF, SQF and QF are coeval for they affect the late Ordovician Mamuniyat Fm. and are parallel in the south of the arch to major faults that are Devonian in age (e.g., Karasek, 1981).

Taken together these observations suggest a fracture history. The earliest fracturing mainly consists in extension fractures across the Cambrian sediments. The Palaeozoic future major faults began to act in the brittle deformation environment of already buried layers but were then minor. Some of them (SAF, CQF, SQF1, SQF2 and SQF3) ceased activity at the end of

the Ordovician. Deformation continued during the middle Palaeozoic and was accompanied by extension fractures in the late Ordovician deposits. A few faults (ASF, NASF and DAF) ended before the latest Ordovician. Activity of major faults that kept-on moving until the late Devonian was accompanied with minor faults (long dykes) in the latest Ordovician Mamuniyat Fm. The rose diagrams of Fig. 10 show that the strikes of the sub-vertical extension fractures (short dykes) remained conspicuously ~E-W during the entire early to middle Palaeozoic. This indicates that the stress field did not significantly change in orientation during this time interval. Evolution of the deformation in Al Qarqaf can be compared to that of Lake Malawi during the Neogene in the East African Rift where brittle deformation was first widespread but progressively concentrated with time into major faults (Chorowicz et al., 1983).

3.2.3.2 Apparent movements

Our mapping shows characteristic geometric patterns that allow components of fault paleo-movements to be inferred in some locations (Dhont et al., 2005). 1) The pattern of en echelon extension fractures along a fault attests to the sense of strike-slip movement (Pollard et al., 1982). For instance SASF in Fig. 9 has a dextral component deduced from the arrangement of right stepping en echelon extension fractures. 2) Rhomb-shaped extensional relay zones clearly indicate the sense of movement of strike-slip faults (Ramsay, 1987), as is the case for the WSW-striking ASF (Fig. 11) that has a dextral component confirmed by slickenside striations measurement in site 19. 3) Local compression may also show sense of movement as illustrated by SSASF bordered by an anticline where the late Cambrian is surrounded in map view by low levels of the early Ordovician (Fig. 5). This is a push-up anticline related to local compression occurring in a left-stepping relay zone of the dextral SSASF. This interpretation is consistent with right-stepping rhomb-shaped structure formed more to the east along the same SSASF (Fig. 5, pa3). 4) The apparent offset of a boundary may be an actual

displacement indicator for instance in Fig. 5 suggesting conjugate sinistral and dextral strike-slip movements respectively along CQF1 and CQF2. 5) Such offsets however are apparent throws and field data are needed. As an example, SASF in Fig. 9 is dextral but apparent offset of the lower Ordovician boundary is left-lateral. 6) Some strike-slip faults have typical tail-crack terminations where extension fractures accommodate horizontal movements (Cruikshank et al., 1991) as is the case for WWF (Fig. 6) that we interpret to be dextral because its south-western end is made of sedimentary dykes filling open cracks.

The overall regional fault system comprises sub-vertical transcurrent faults (Fig. 10): 1) dextral N55°E to N65°E (N60°-family); 2) sinistral N80° to 110°E (N90°-family). Major ~N-striking faults with a vertical throw component run in the central and northern study area but exact mechanisms could not be determined from the satellite images alone.

3.2.4 Field fault structural analysis

We measured the dip and strike of fault planes and sense of movement at each fault we could get to, basing our observations mainly on gouge movement indicators such as Riedel fractures, striations, quartz or crushed sandstone steps or layer offsets. This approach suits remote sensing fault mapping whereas strain inversion methods generally used for determining local paleo-stress components are mainly based on the statistical analysis of a great number of minor faults that cannot be mapped. We plot the field measurements in lower hemisphere Schmidt diagrams for each site (e.g., Fig. 12).

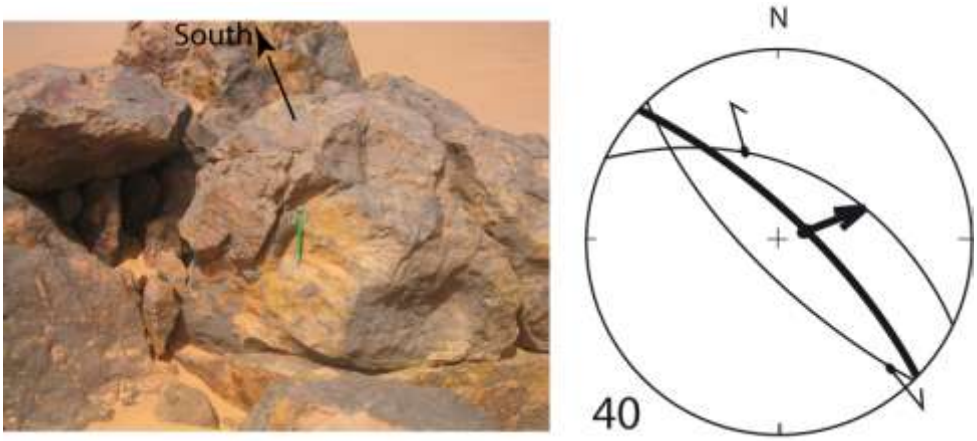

Figure 12. Plot of dip and strike of fault planes of the Mamuniyat fault zone (MF) at site 40 located in Fig. 10. Pitch and sense of movement according to striations. This Schmidt diagram lower hemisphere indicates that the movement along the major fault (thick line and arrow) is extensional; minor faults (thin line semi-arrows) advocate strike-slip strain components. Explanation of symbols in legend of Fig. 13.

The main fault at each site is that we have mapped from the space. The dip and strike was estimated from satellite imagery and/or field check. The main fault plane sometimes can be identified and measured in outcrop but is not always obvious. However, faults that are parallel to each other at a given site and relate to the same event might have the same mechanism. We consequently assumed that movement along the main fault is that of nearby minor planes of similar dip and strike. We graphically illustrated movements in the plots by symmetric arrows or semi-arrows, centripetal for compression, centrifugal for extension (Figs. 11, 12, 13 and 14).

We could not directly observe the main fault plane or any nearby minor striated plane parallel to it at sites 21, 43 (Fig. 13) and 52 (Fig. 14). Layers dipping SW54° and striking N160°E of site 43 are consistent with local fold accompanying the Mamuniyat normal fault, western side down (Fig. 10, MF). The N60° and N90° fault families are dextral in sites 19 (Fig. 11), 26, 27,

28, 29, 30, 44, 46, 47 (Fig. 13) and 51, 53, 54, 55, 56, 57, 59, 60, 61, 62, 64, 65 (Fig. 14). The movements deduced from mapping along ASF, SSASF and QF (Fig. 10) are confirmed. Measurements in site 58 (Fig. 14) are consistent with the N100°E-striking sinistral SQF3, and in sites 21, 28, 44, 46, 54 (Figs. 13 and 14) with sinistral NW-SE faults. Sites 36, 37 (Fig. 13) and 63 (Fig. 14) confirm that the major ~N-striking faults are extensional. Other major faults are extensional dextral oblique-slip in sites 20 and 33 (Fig. 13). At site 20 a N70°E-striking fault borders a rhomb-shaped pull-apart feature. A few reverse components occur along strike-slip faults in sites 24, 29, 45, 47 (Fig. 13) and 48, 61, 64 (Fig. 14). It is common to find local compression along high angle strike-slip faults when there is a bend in the fault plane that may cause a push-up structure as is the case for sites 24 and 45 along respectively the SSASF and its western prolongation between the ADF and MF faults (Fig. 10). Sites 27, 28, 29 and 30 (Fig. 13) express almost pure dextral strike-slip motion along the Tmisan fault (TF) forming the southern border of Al Qarqaf (Fig. 10).

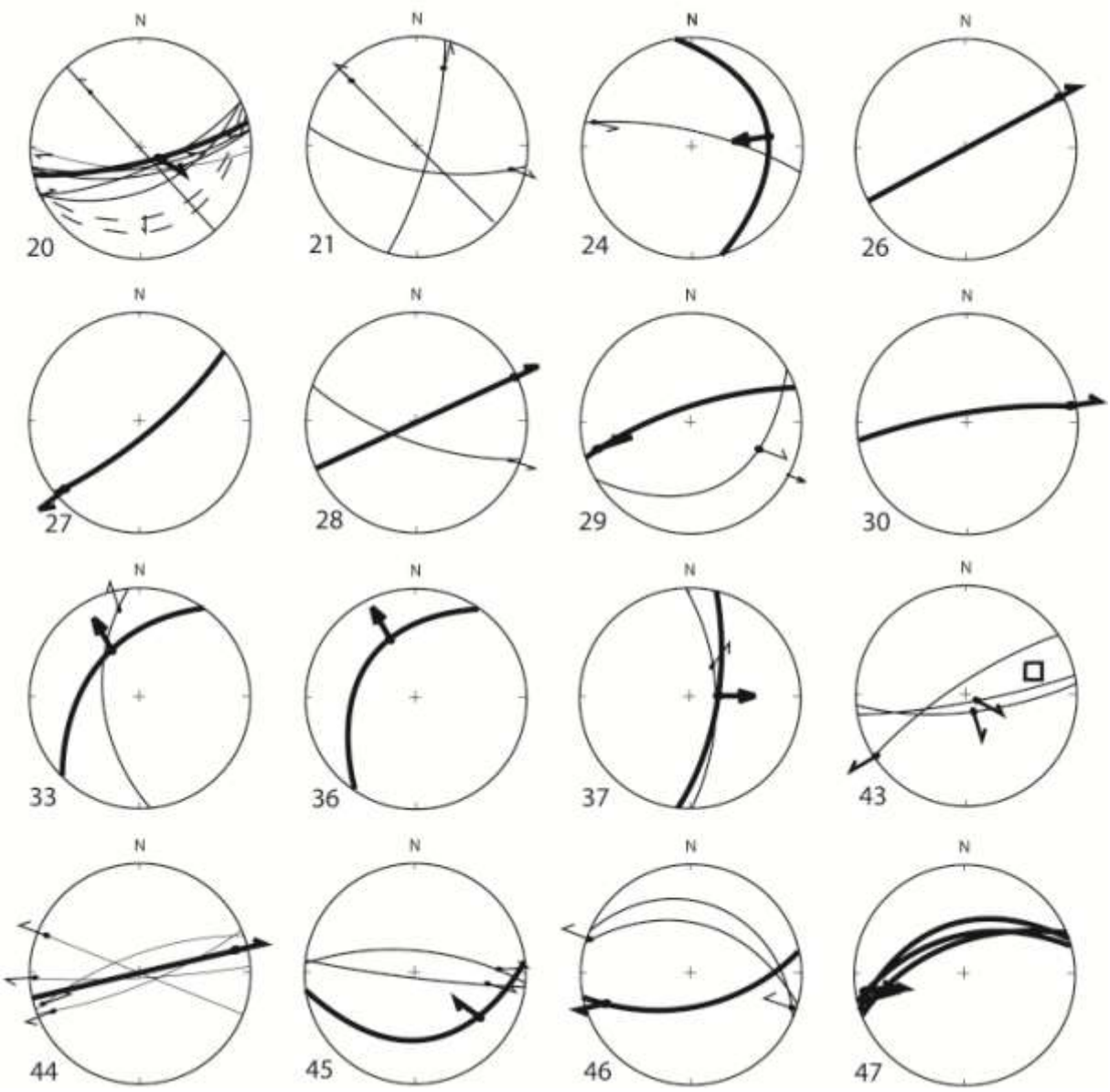

Figure 13. Plots of field structural measurements along faults at sites 20 to 47. See Fig. 10 for site location. Schmidt projection, lower hemisphere. Thin or thick lines and arrows respectively represent minor or major mapped faults and related striations with observed sense of movement. Symmetric centrifugal arrows represent almost pure extension. Semi-arrows express dextral or sinistral strike-slip movement components. Square is pole of stratigraphic plane.

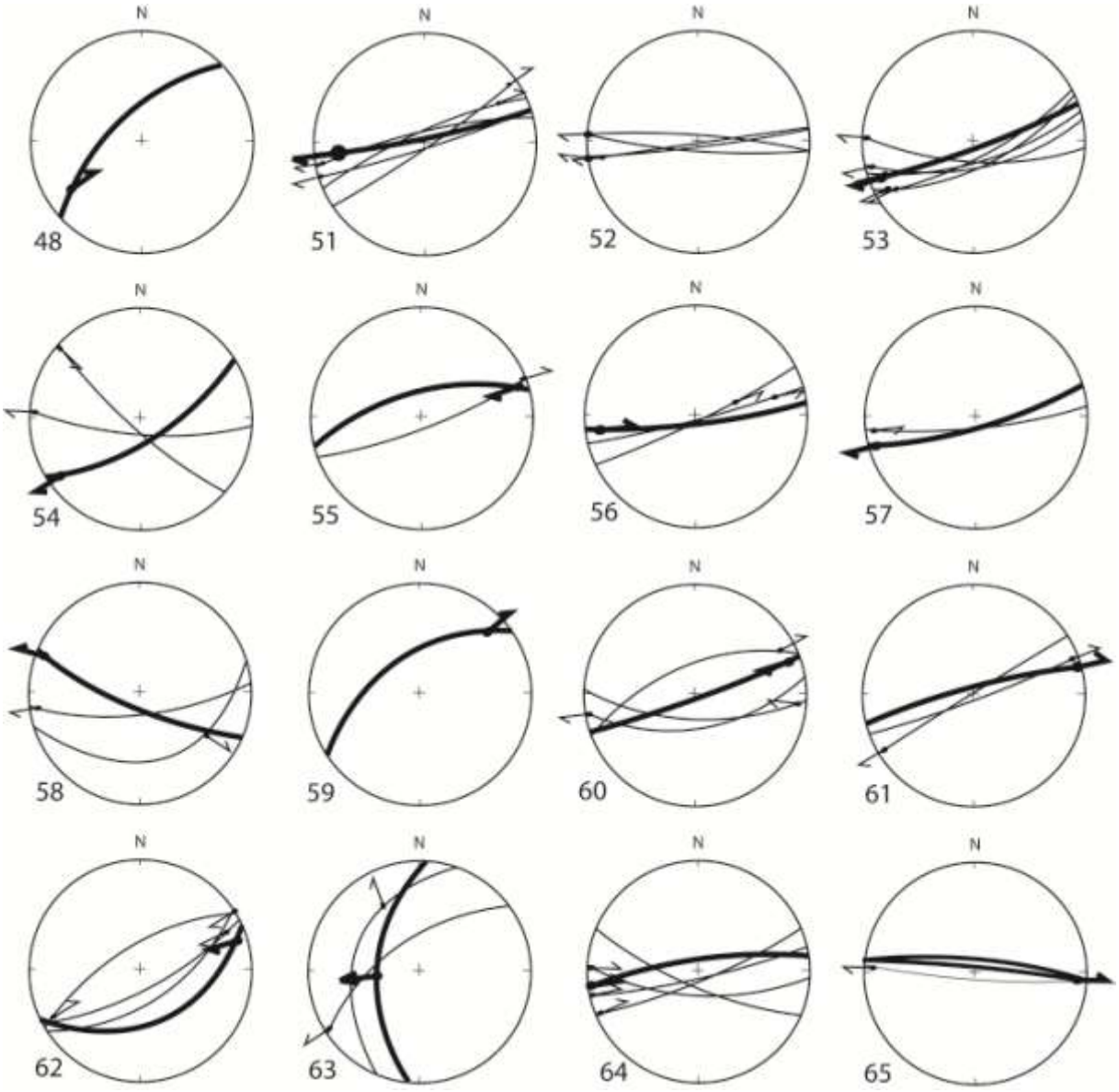

Figure 14. Plots of field structural measurements along major faults at sites 48 to 65. See Fig. 10 for site location. Schmidt projection, lower hemisphere. Thin or thick lines and arrows respectively represent minor or major faults and related striations with observed sense of motion. Symmetric centrifugal arrows represent almost pure extension. Semi-arrows express dextral or sinistral strike-slip movement components.

We copied onto the map of Fig. 10 at each site the horizontal component of main fault movement from structural analysis diagrams. Strike-slip mechanisms are consistent with those

deduced from mapping: the N60°-family is dextral, the N90°-family sinistral. The main result from field structural analysis is that the ~N-S family is actually extensional or tensional oblique-slip. Mechanisms of major faults are now known from mapping, image interpretation and field structural analysis. They demonstrate that the Qarqaf arch at its western end is part of a dextral ~N75°E-striking fault zone. This is almost the strike of the longest faults in it (N60°-family) and of the dextral en-echelon bordering faults at its southern rim. The Qarqaf arch is thus a right-lateral transcurrent fault zone, also comprising a left-lateral N90°-family.

The ~N-striking normal faults (MF and ADF in Fig. 10) border late Ordovician outcrops of the Wadi Ash Shabiyat graben block (cross-section XY in Fig. 4). The Bir Aishah anticline located west of the ADF with axis parallel to it then is not formed by compression but must be interpreted as a fold related to normal faulting. This is a tectonic style along tilted blocks in extensional environment similar for example in the Gulf of Suez rift to drag folds (Chorowicz et al., 1986) or perhaps fault-propagation folding (Sharp et al., 2000). Such extensional structures inside a strike-slip fault zone are understandable considering the Qarqaf fault (QF, Fig. 10) is a dextral lateral ramp ending to the west into listric normal faults with arcuate trace, in a sort of half-spoon fault system (see insert in Fig. 10). This tectonic style is analogous to the half-spoon fault tectonics inside the Tanganyika-Rukwa-Malawi strike-slip fault zone bordering the north-western end of Lake Malawi rift in Eastern Africa (Chorowicz and Sorlien, 1992).

4 Regional structural style

4.1 Depocentres and paleo-transfer fault zone

The Qarqaf arch was during the Palaeozoic then part of a right-lateral strike-slip fault zone between the Ghadamis and Murzuq basins that both were forming by extension since the Cambrian (Ziegler, 1988; Kröner, 1991; Scotese et al., 1999 and Hallett, 2002). The Ghadamis and Zamzam depocentres in the north and the Murzuq one in the south were

distinct during the Cambro-Ordovician but vanished during the Devonian (Fig. 15). Their NNW-SSE elongate shape is of almost 500 km in length and more than 200 km in width with a distance of 550 km separating the axes of two depocentres in the Ghadamis basins. Such dimensions suggest they were large graben structures in a continental rift system, similar to segments of the East African Rift (Chorowicz, 2005) and the Rhinegraben (Bergerat and Chorowicz, 1980; Chorowicz and Deffontaines, 1993) but subsidence due to dynamic topography is not excluded (Heine et al., 2008).

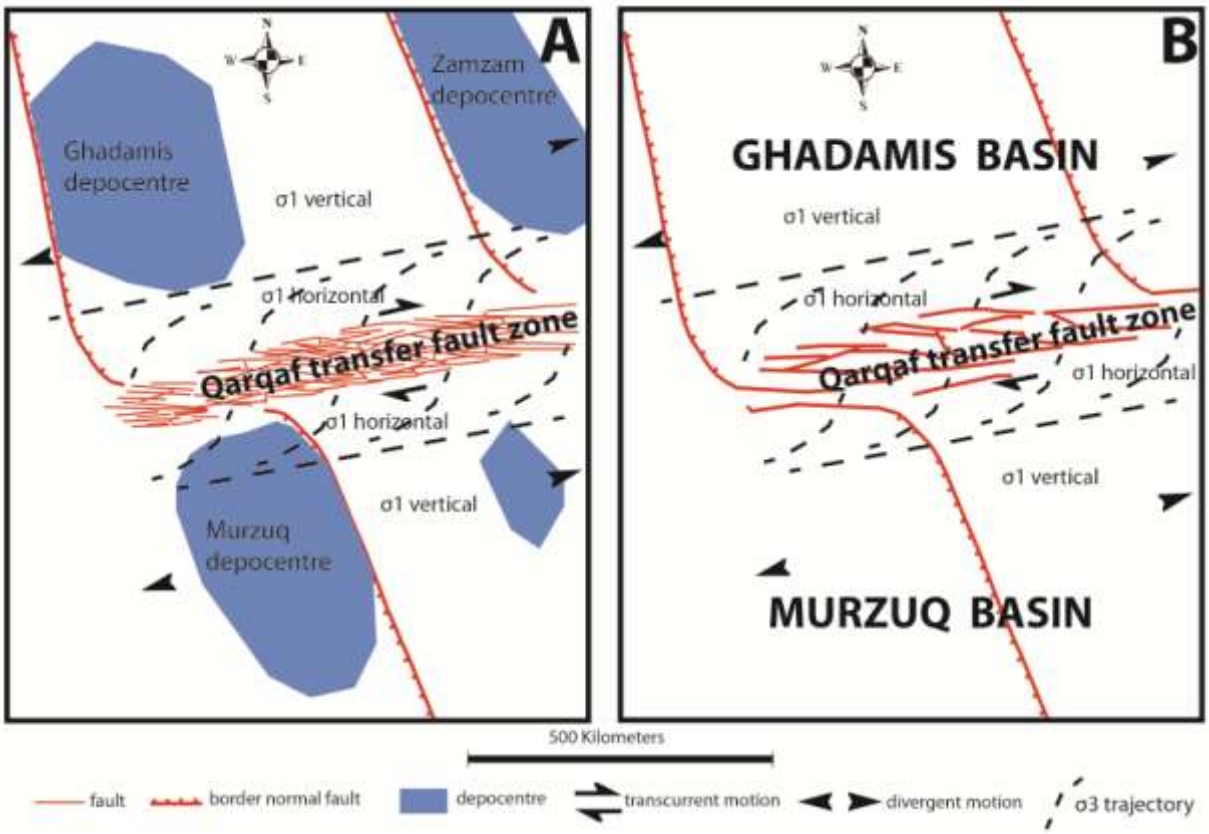

Figure 15. Map model of the Qarqaf arch geodynamics during the Palaeozoic. A: Cambrian-lower Ordovician paleogeography (Hallet, 2002) and schematic inferred fault set. B: Devonian schematic fracturing. σ1 and σ3 are trajectories of maximum and minimum stress components that we have observed in the fault zone (~NS, at right angle to the vertical E-striking extension fractures) but inferred on both sides in the basins.

The tectonic style consisted in Palaeozoic graben structures linked by a transfer fault arch that developed together with the rifting process. This tectonics started with numerous small active faults and joints during the Cambrian and continued until the late Devonian while the deformation progressively focused into a few major faults. A similar style of deformation with graben basins separated by strike-slip transfer faults was occurring in the Congo basin at the same time (Deffontaines and Chorowicz, 1991).

Rifts structures generally are asymmetrical subsiding areas with a major border fault zone running along one side. We have applied this scheme in Fig. 15. Transfer faults are often accompanied by reversal in graben asymmetry (Chorowicz, 2005). We infer by analogy and from the occurrence of the extensional NS-striking Mamuniyat and Qarqaf faults that opposite half-spoon faults were connected by the transfer fault zone and prolonged northward or southward to form the major border faults of the depocentres thus determining their sense of asymmetry (Fig. 15).

4.2 Arch genesis

Our interpretation in terms of transfer fault zone in rift structure permits to understand the arch uplift. The stress field along strike-slip faults is supposed to have maximum ($\sigma 1$) and minimum ($\sigma 3$) stress components both horizontal. But in nearby basins $\sigma 1$ should have rotated to vertical and be responsible for the subsidence while $\sigma 3$ remains horizontal (Fig. 15). A transfer fault zone does not necessarily extend beyond the segment where it links graben structures, as is the case in Fig. 15. The pronounced western closure of the Qarqaf arch is one end of the paleo-transfer fault zone.

Testing the transfer fault model necessitates to collect more data about the paleo-stress field in Al Qarqaf region. The ~E-W short sedimentary vertical dykes (Fig. 10) already indicate a

horizontal ~N-S trending σ3, i.e. at right angle to these extension fractures. Such a horizontal σ3 is consistent with the N55°E to N65°E dextral and the N80°E to N100°E sinistral major strike-slip faults. Close to strike-slip faults usually σ1 and σ3 are both horizontal and σ2 (mean stress component) is vertical. This stress field is expected to locally rotate when approaching the extensional faults of the spoon fault systems with σ1 rotating to vertical but this awaits further fieldwork. We have no structural analysis data in the nearby basins and our hypothesis is that the paleo-stress field was there extensional with σ1 vertical and σ3 horizontal progressively approaching to N75°E-trend as the distance to the arch increased (Fig. 15). This should be checked from drill core samples and further field structural analysis.

5 Discussion

5.1 Folds in the Devono-Carboniferous

Our observation of fold related to normal fault and generalized Palaeozoic extension linked to strike-slip regime contradicts the description by Glover et al. (2000) of compressive folds in Devonian outcrops and our mapping of other folds in the Carboniferous immediately northwest of the arch (Fig. 16). Sub-horizontal late Mesozoic-early Paleogene carbonates in this area unconformably lay over the early Carboniferous Marar Fm., a ~800 m thick sequence grading from shale to silty shale and sandstone (Whitbread and Kelling, 1982) that disconformably rests on the late Devonian Dabdab Fm. and is overlain by the late Carboniferous Assed Jefar and Dembaba Fms. (Fig. 16B). The Marar outcrops are dark purple in the standard coloured Landsat imagery and display cuesta successions that correspond to sandstone layers (Fig. 16A). The unit on the whole forms a monocline structure dipping NW ~5° but closures of bedding traces to the west permit to deduce fold axes that trend WNW-ESE, turning eastward to WSW-ENE (Fig. 16B).

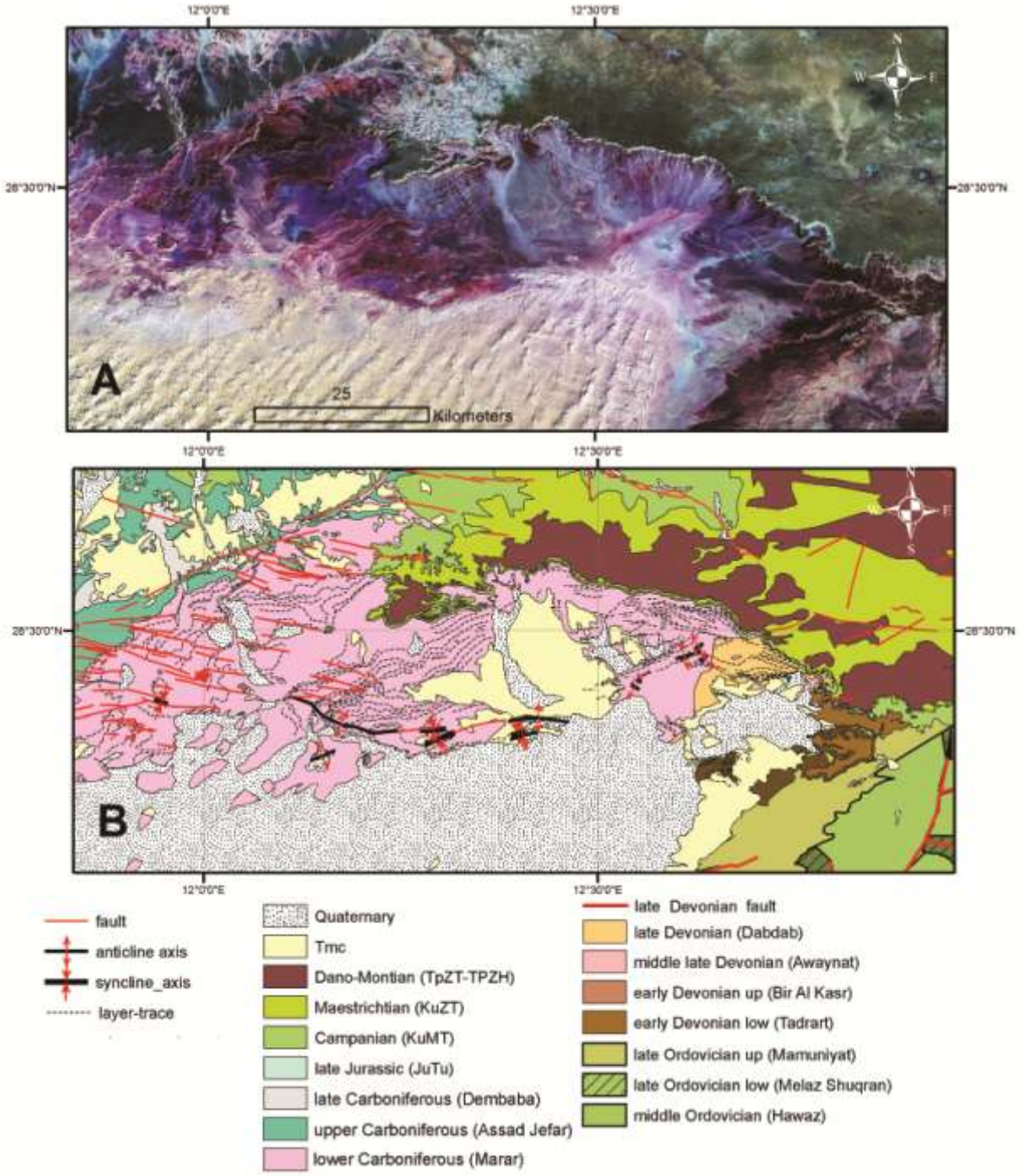

Figure 16. Updated geological map of Northwestern Al Qarqaf. Location in Figure 1. A: standard colour composite image of Landsat ETM+ data (blue, band 1; green, band 3; red, band 5). B: new mapping using ERS SAR imagery for more bedding traces. Closures of bedding traces permit to deduce fold axes.

Several hypotheses can be explored to explain these folds: general or local compression, slumping, normal faulting and related folds, collapse structures. Fold axes trend more or less parallel to the axis of the Qarqaf arch but cannot be regarded as its western prolongation because they do not lie along the arch axial line (Fig. 1) and are not straight (Fig. 16). We did not find any associate strike-slip fault. Glover et al. (2000) have described in the western end of the arch closure Devonian layers affected by extensional listric growth faults and associated compressional leading edge folds including sheath folds. They deduced that soft deposits slid at the end of their deposition over the uplifting and tilting monoclinal Devonian layers.

We acknowledge their view and also consider the folds in the Carboniferous to result from a Carboniferous gravity sliding effect unrelated to strike-slip tectonics or regional compression. This interpretation implies that compression occurred only inside the local sliding mass. This is not contradictory with the regional tectonic model of trans-tensional deformation responsible for arch uplift. A seismic profile across the plateau shows in Devono-Carboniferous layers local loss in continuity that can be regarded to result from décollement and gravity sliding above the more regular monocline of the early Palaeozoic units (Fig. 17).

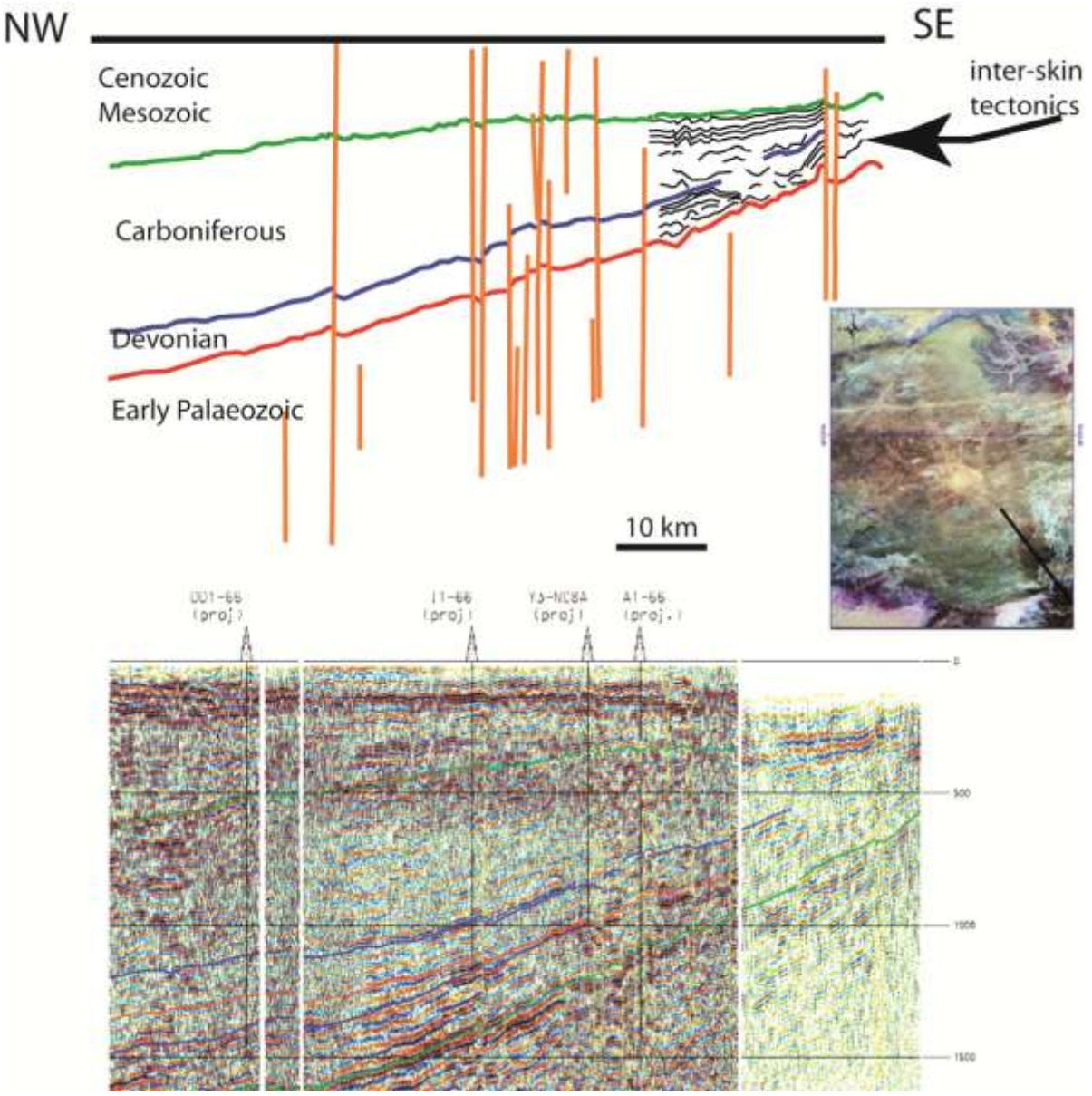

Figure 17. Seismic profile across the plateau in the eastern inferred prolongation of the Carboniferous outcrops. Location of profile is inserted in a Landsat image. Our interpretation of the tectonic style is disharmonic folding related to local décollement during the Carboniferous. Vertical lines in cross-section are faults interpreted from profile. Source of profile and analysis: Libyan Petroleum Institute (Tripoli).

5.2 No Palaeozoic compression event

The identification of the tectonic events that are responsible for the arch formation is disputed. The Panafrican late Proterozoic compressive event was implicated (Montgomery, 1994) but the arch also affects the Palaeozoic series. The Caledonian (late Silurian-early Devonian) orogeny is sometimes taken into consideration (e.g., Said and Kanes, 1985). This event is documented in Al Qarqaf by stratigraphic unconformities attesting to a 'Caledonian' (in age) beginning of the Devonian sedimentary cycle accompanied by regional extension (Derder et al., 2015) but no compressive structures occurred at that time.

A compressional 'Variscan (Hercynian)' orogeny is sometimes supposed to have affected the area (e.g., Klitszch, 2000; Carruba et al., 2014). But there is no evidence in the studied area of such a regional compression. The only shortening structures observed are local push-up deformations along strike-slip faults and gravity sliding folds in the Devono-Carboniferous. The Bir Aishah fold described in this paper is in fact a drag fold or a fault propagation fold accompanying extensional movement along a normal fault. Klitzsch (1970) stated that extension began in the early Palaeozoic and our observations show that it was part of basins evolution starting from a rift system and associated with a crosscutting transfer fault zone but it was not followed by compression in the late Palaeozoic. The arch can be better explained by the transfer fault model implying long duration extension and associate transcurrent movements during the Palaeozoic. The global scale view of Stampfli and Borel (2002) shows the lack of a Variscan collision in the study area.

There is however a large regional 'Variscan (Hercynian)' unconformity in Libya (e.g., Echikh, 1992, 1998; Boote et al., 1998; Scotese et al., 1999; Hallet, 2002). Seismic profiles of the Libyan Petroleum Institute database illustrate this feature (Fig. 18) but a careful analysis of Fig. 18 shows that dated Carboniferous formations are upward followed by conformable layers which may relate to the Permian but no age has been yet affected. We infer that the

regional event related to large regional disconformity is not the late Carboniferous 'Variscan' (in age) one but the well known Triassic event of opening of the Neo-Tethys. This speculation needs further work on drill cores, which would be a good test but these data are not presently available to us.

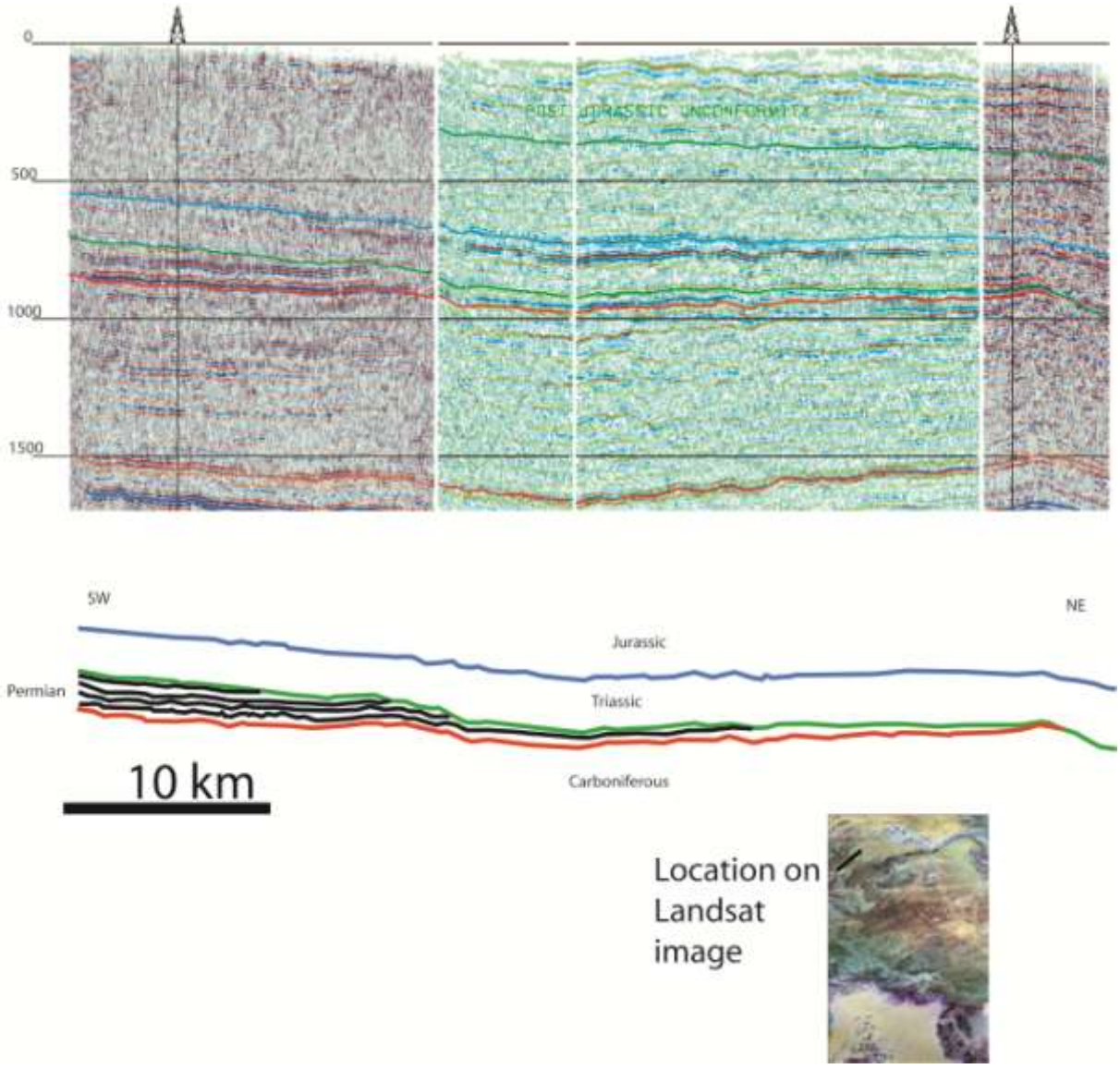

Figure 18. Seismic profile located north of the study area (source and analysis, Libyan Petroleum Institute, Tripoli), accompanied by two drill projects. The layers we have copied in black into the scheme at bottom of this figure are located between the late Carboniferous (Dembaba Formation, roof drawn in red) and the Triassic rocks (base in green, roof in blue)

might be ascribed to the Permian. We speculate that these supposed Permian layers together with the late Carboniferous are cut by the unconformity (in green), which consequently postdates the Carboniferous and the Permian and should be related to the early opening of the Neo-Tethys.

5.3 Tectonic reactivation

The N60°, N105° and N10° short fault families that cut Carboniferous and Mesozoic layers (Fig. 16) strike almost the same than the Palaeozoic N60°, N90° and N165° families. This suggests that post-Palaeozoic local reactivation of previous faults has occurred. We however never found in the field several striation families along fault gouges.

The Palaeozoic fractures taken together form a coherent system of deformation consistent with the transfer fault zone model but not significantly disturbed by a more recent system. The opening of the Neo-Tethyan Ocean since the Triassic yet induced extensional tectonics but this extension is limited in the study area (Conant and Goudarzi, 1967). A late Cretaceous compression episode in northern Africa had induced tectonic inversion structures, notably in Cyrenaica (Libya) and the Western Desert of Egypt (Guiraud and Bosworth, 1997; Guiraud, 1998; Bosworth et al., 2008). It is true that late Cretaceous-Paleocene carbonate layers are slightly folded in the Hammadah al Hamra plateau close to our study area (Fig. 1). A noticeable event forming the Hon graben and characterized by N160°E-striking faults (Fig. 1) occurred during the Paleogene (Abadi, 2002; Jerzykiewicz et al., 2003) but Al Qarqaf region seems out of this graben influence. Miocene to Quaternary alkaline volcanism formed out of the study area in the eastern part of Al Qarqaf. No collisional event occurred during the Mesozoic-Cenozoic times (Said and Kanes, 1985; Montgomery, 1994).

5.4 Consequences for oil exploration

Consequences of our observations for oil exploration (Sikander, 2000; Al Fasatwi, 2001) remain a research subject. New extensive compilation of the geologic data existing about Al Qarqaf and adjacent basins should be done. Subsidence, uplift, thermal history of arch and basins and timing of hydrocarbon generation and migration should take into account that no regional compression occurred during the Palaeozoic. Porosity data, burial and structural diagenesis history should be examined on the basis that long duration of overall extensional and strike-slip strain have facilitated high porosity to be maintained in sandstones with effects on fluid migration.

We have here argued that the main regional disconformity in Northern Libya is of Neo-Tethyan age, not Variscan. If later confirmed by drilling (Fig. 18), this would help exploration strategies to be undertaken and more precise reading of seismic profiles to be performed. Our model of distribution and age of fault systems is a key issue for geometric basinal analysis of traps distribution in the Ghadamis and Murzuq basins. Faults related to syn-depositional extension in rift basins generally control local variations in sediment facies and thickness, as demonstrated by Adamson et al. (2000) in the Murzuq basin. Our model should help finding these variations along major normal faults. Low angle unconformities and thinning of units should appear at any level as an effect of continuous fault activity and its focus with time. It was often admitted that most folds in the region are due to compression during Variscan orogeny but they rather are related to folding along normal faults. This is already known for the major 'Elephant' discovery in the Murzuq basin (Davidson et al., 2000). Such gentle folds with axial length of several tens of kilometres are a major target for exploration. The occurrence of roll-over bending in down-thrown compartment of spoon fault configurations is not excluded and may be interpreted from seismic profiles. Other folds comprise local 1-2 km long and 1 km wide anticlines related to push-up relay zones. They should be evidenced along

~E-W strike-slip faults in positive flower arrangements. Pull-apart features of similar dimensions along these faults may also provide fault traps of negative flower style. Strike-slip faults along the Qarqaf arch are supposed to prolong far in depth, rooted on Panafrican structures whilst normal rift faults are listric. Gravity sliding of soft sediments in the Devono-Carboniferous is responsible for gentle irregular 1 or 2 km wide and ~10 km long folds that may form traps.

6 Conclusions

The structural style of the N75°E-trending Qarqaf arch during the Palaeozoic is that of a right-lateral strike-slip fault zone between the Ghadamis and Murzuq basins. We refer to a model of transfer fault zone along the Qarqaf arch, accommodating the formation of rift basins on both sides. The fault zone comprised dextral N55°E to N65°E faults and sinistral N80°E to N100°E faults and included ~N-striking normal faults connected to ~E-striking dextral lateral ramps. The fracturing began during the Cambrian in extensional strike-slip environment and formed openings that were immediately filled to later express as sedimentary dykes. The early fracturing was widespread but relative displacements progressively focused into a few faults during the Cambrian to Devonian time. The anticlinorium structure was acquired progressively through that time, a strike-slip fault zone being less subsiding than the adjacent rift basins. The border normal faults of the graben depocentres were possibly connecting to the paleo-transfer fault, with a change in graben asymmetry across the zone. Such tectonics gave way in the basins to subsequent continental thinning, rift thermal evolution and finally to long duration basin genesis throughout the Palaeozoic.

The transfer fault zone model implies that the regional Palaeozoic geodynamics is relative to tensional environment. Compressive folds in Devono-Carboniferous formations at northwest end of Al Qarqaf are due to gravity sliding of soft material along the northern slope of the uplifting paleo-transfer fault zone. Other folds in the area are local push-up relay zones along

strike-slip faults or folds related to normal faulting. No structures of a large Variscan (Hercynian) compressional belt have been found. A so call 'Variscan' regional disconformity seems not to be of late Palaeozoic age but rather related to the well known Triassic opening of the Neo-Tethys.

Our methodology for updating geologic maps combines the use of satellite imagery with field work and structural analysis. Results concerning the fault mechanisms by both methods are consistent. Our mapping has provided relevant precise discoveries such as the evidencing of the Wadi Ash Shabiyat graben, the Bir Aishah anticline and the classification of fracture sets.

7 References cited

Abadi, A., 2002. Tectonics of the Sirt basin. Netherlands Research School of Sedimentary Geology (NSG), publication n° 20011203, PhD thesis Delft Technical University, ITC Dissertation n° 90, ISBN 90-6164-205-1, 187p.

Adamson, K., Glover, T., Whittington, R., Craig, J., 2000. The Lower Devonian succession of the Murzuq Basin – possible indicators of eustatic and tectonic controls on sedimentation, in: Sola, M.A., Worsley, D. (Eds.), Geological Exploration in Murzuq Basin. Elsevier Science, pp. 431-447.

Al Fasatwi, Y.A., 2001. The structural, paleogeographical and hydrocarbon systems analysis of the Ghadamis and Murzuq basins, West Libya, with special emphasis on their relation to the intervening Al Qarqaf Arch. Promotor(s) K.J. Weber and P.M. van Dijk, Enschede: PhD thesis Delft Technical University (ITC Dissertation n° 83), ISBN 90-6164-198-5, 199p.

Al Fasatwi, Y.A., Van Duk, P.M., Erren, J.W.M.G., 2003. Surface and subsurface characteristics of Al Qarqaf Arch and adjacent parts of the Ghadamis and Murzuq basins, West Libya: an integration of remote sensing, aeromagnetic and seismic

interpretation, in: Salem, M.J., Oun, K.M., Seddiq, H.M. (Eds.), The Geology of Northwest Libya. National Library, Benghazi, Libya 3, 171-190.

Banerjee, S., 1980. Stratigraphic Lexicon of Libya. Industr. Res. Cent, S.P.L.A.J., Tripoli, 13, 176 p.

Bardintzeff, J.-M., Deniel, C., Guillou, H., Platevoet, B., Telouk, P., Oun, K.M., 2011. Miocene to recent alkaline volcanism between Al Haruj and Wawan Namous (southern Libya). International Journal of Earth Sciences 101, 1047–1063.

Becker, S.P., Eichhubl, P., Laubach, S.E., Reed, R.M., Lander, R.H., Bodnar, R.J., 2010. A 48 m.y. history of fracture opening, temperature, and fluid pressure: Cretaceous Travis Peak Formation, East Texas basin. Geological Society of America 122(7-8), 1081-1093.

Belhaj, F., 1996. Palaeozoic and Mesozoic stratigraphy of eastern Ghadamis and western Sirt Basins, in: Salem, M.J., Mouzughi, A.J., Hammuda, O.S. (Eds.), The Geology of Sirt Basin. Elsevier, Amsterdam I, 57-96.

Belhaj, F., 2000. Carboniferous and Devonian stratigraphy - the M'rar and Tadrart reservoirs, Ghadames Basin, Libya, in: Sola, M.A., Worsley, D. (Eds.), Geological Exploration in Murzuq Basin. Elsevier Science B.V., 117-142.

Bellini, E., Massa, D., 1980. A stratigraphic contribution to the Palaeozoic of Southern basins of Libya, in: Salem, M.J., Busrewil, M.T. (Eds.), Geology of Libya (I). Academic Press, London, pp. 3-56.

Bergerat, F., Chorowicz, J., 1980. Etudes des images Landsat de la zone transformante Rhin-Saône (France). Geologische Rundschau 70(1- 2), 354-367.

Billo, S.M., 1985. The Transcontinental Arch and its relation to Colorado oil and mineral belt. Journal of Petroleum Geology 8(3), 343-352.

Bishop, W.E., 1975. Geology of Tunisia and adjacent parts of Algeria and Libya. America Association of Petroleum Geologists Bulletin 59(3), 413-450.

Blanpied, C., Deynoux, M., Ghienne, J.-F., Rubino, J.-L., 2000. Late Ordovician glacially related depositional systems of the Gargaf Uplift (Libya) and comparisons with correlative deposits in the Taoudeni Basin (Mauritania), in: Sola, M.A., Worsley, D. (Eds.), Geological Exploration in Murzuq Basin. Elsevier Science, 485-507.

Bonnefous, J., 1963. Synthèse stratigraphique sur le Gothlandien des sondages du Sud Tunisien. Revue de l'Institut Français du Pétrole, 18(10/11), 123-133.

Bosworth, W., El-Hawat, A.S., Helgeson, D.E., Burke, K., 2008. Cyrenaican "shock absorber" and associated inversion strain shadow in the collision zone of northeast Africa. Geological Society of America Bulletin 36(9), 695-698.

Boote, D.R.D., Clark-Lowes, D.D., Traut, M.W., 1998. Palaeozoic petroleum systems of North Africa, in: Macgregor, D.S., Moody, R.T.J., Clark-Lowes, D.D. (Eds.), Petroleum Geology of North Africa. Geological Society, London, Special Publication 132, 7-68.

Burchfiel, B.C., Stewart, J.H., 1966. "Pull-apart" origin of the central segment of Death Valley, California. Geological Society of America Bulletin 77, 439-442.

Burollet, P.F., 1960. Lexique stratigraphique international Vol. IV Afrique, Fasc. IVa Libye, 62 p. Congrès Géologique International, Centre National de la Recherche Scientifique, Paris.

Burollet, P.F., Manderscheid, G., 1967a. Le Dévonien en Libye et en Tunisie. International symposium on Devonian System, 1, 205-213, Calgary, Canada.

Burollet, P.F., Manderscheid, G., 1967b. General Geology of Tunisia. Guidebook to the geology and history of Tunisia. Petroleum Exploration Society, Libya, 9th annual field conference 215-225.

Carruba S., Perotti C., Rinaldi M., Bresciani I., Bertozzi G., Intraplate deformation of the Al Qarqaf Arch and the southern sector of the Ghadames Basin SW Libya), Journal of African Earth Sciences 97, 2014, 19-39.

Castro, J.C., Della Favera, J.C., El-Jadi, M., 1985. Palaeozoic sedimentary facies, Murzuq basin. S.P.L.A.J. International Report Braspetro-Petrobras, Rio de Janeiro, 117 p.

Chorowicz, J., 1980. Mise à jour de notions utilisées par les géologues en télédétection. Comptes Rendus sommaires de la Société géologique de France 5, 203-206.

Chorowicz, J., 2005. The East African Rift System, Journal of African Earth Sciences 43(1-3), 379-410.

Chorowicz, J., Deffontaines, B., 1993. Transform faults and pull-apart model in the Rhinegraben from analysis of multisource data. Journal of Geophysical research 98(B814), 14339-14351.

Chorowicz, J., Deroin, J.-P., 2003. La télédétection et la cartographie géomorphologique et géologique. Editions Gordon & Breach, collection Geosciences 141 p.

Chorowicz, J., Dhont, D., Ammar, O., Rukieh, M., Bilal, A., 2004. Tectonics of the Pliocene Homs basalts (Syria) and implications for the Dead Sea Fault Zone activity. Journal of the Geological Society, London 162, 259-271.

Chorowicz, J., Henry, C., Lyberis, N., 1986. Tectoniques superposées synsédimentaires des secteurs des golfes de Suez et d'Aqaba. Bulletin de la Société géologique de France 8, I(2), 223-234.

Chorowicz, J., Le Fournier, J., Le Mut, C., Richert, J.P., Spy- Anderson, F.L., Tiercelin, J.J., 1983. Observation par télédétection et au sol de mouvements décrochants NW-SE dextres dans le secteur transformant Tanganyika-Rukwa-Malawi du Rift Est-Africain. Comptes Rendus de l'Académie des Sciences de Paris II, 296, 997-1002.

Chorowicz, J., Sorlien, C., 1992. Oblique extensional tectonics in the Malawi Rift. Geological Society of America Bulletin 104, 1015-1023.

Collomb, G.R., Heller, C., 1958/1959. Etude géologique de la bordure occidentale du bassin de Mourzouk. Unpublished report, Compagnie Petrole TOTAL 30p.

Conant, L.C., Goudarzi, G.H., 1967. Stratigraphic and tectonic framework of Libya. A.A.P.G., Bull. 51, 719-730.

Craig, J.C., Rizzi, F., Said, B., Thusu, S., Lüning, A.I., Asbali, M.L., Keeley, J.F., Bell, M.J., Durham, M.H., Eales, S., Beswetherick, S., Hamblett, C., 2008. Structural styles and prospectivity in the Precambrian and Paleozoic hydrocarbon systems of North Africa. Geology of East Libya 4, 51-122, in: Salem, M.J., the Geology of East Libya. Third Symposium on the Sedimentary Basins of Libya, Benghazi, November 11-13, 2004.

Cruikshank, K.M., Zhao, G., Johnson, A.M., 1991. Analysis of minor fractures associated with joints and faulted joints. Journal of Structural Geology 13, 865-886.

Dautria, J.M., Lesquer, A., 1989. An example of the relationship between rift and dome: recent geodynamic evolution of the Hoggar swell and of its nearby regions (Central Sahara, Southern Algeria and Eastern Niger). Tectonophysics 163, 45-61.

Davidson, L., Beswetherick, S., Craig, J., Eales, M., Fischer, A., Himmall, A., Jho, J., Mejrab, B., Smart, J., 2000. The structure, stratigraphy and petroleum geology of the Murzuq basin, Southwest Libya, in: Sola, M.A., Worsley, D. (Eds.), Geological Exploration in Murzuq Basin. Elsevier Science, pp. 295-320.

De Castro, J.C., Della Favera, J.C, El Jadi, M., 1985. Palaeozoic sedimentary facies, Murzuq basin. S.P.L.A.J. International Report Braspetro-Petrobras, Rio de Janeiro, 117p.

Deffontaines, B., Chorowicz, J. 1991. Principle of hydrographic network analysis from multisource data. Application to structural analysis of the Zairian basin. Tectonophysics 194, 237-263.

Derder, M.E.M., Maouche, S., Liégeois, J.P., Henry, B., Amenna, M., Ouabadi, A., Bellon, H., Bruguier, O., Bayou, B., Bestandji, R., Nouar, O., Bouabdallah, H., Ayache, M., Beddiaf, M., 2015. Discovery of a Devonian mafic magmatism on the western border of the Murzuq basin (Saharan metacraton): paleomagnetic dating and geodynamical implications, Journal of African Earth Sciences, doi: 10.1016/j.jafrearsci.2015.11.019.

Desio, A., 1936. Riassunto sulla constituzione geologica del Fezzan. Bolletino della Societa geologie a Italiana 55 (2), 319-356.

Desio, A., 1960. Lexicon of stratigraphy for Libya. Petroleum Exploration Society of Libya, 157pp.

Dhont, D., Chorowicz, J., Collet, B., Lichtenegger, J., Barbieri, M., 2005. Space borne radar applications in geology. An introduction to imaging radar, and application examples of ERS SAR in Geology and Geomorphology. The European Space Agency, ESA Publications Division, ESTEC, Noordwijk, the Netherland TM-17, 230 p.

Echikh, K., 1992. Geology and hydrocarbon potential of Ghadamis basin. Internal Report, National Oil Company of Libya (NOC), Tripoli.

Echikh, K., 1998. Geology and hydrocarbon occurrences in the Ghadames Basin, Algeria, Tunisia, Libya, in: Macgregor, D.S., Moody, R.T.J., Clark-Lowes, D.D. (Eds.), Petroleum Geology of North Africa. Geological Society, London, Special Publication 132, 109-130.

El-Mehdawi, A.D., 2000. Palynological analysis of the lower Acacus member in wells A1-NC1 and A1-NC3A, Ghadamis basin, NW Libya, in: Salem, M.J., Khaled, M.O. (Eds.), The Geology of Northwest Libya. National Library, Benghazi, Libya 1, 225-236.

Elshaafi, A., Gudmundsson, A., 2016. Volcano-tectonics of the Al Haruj Volcanic Province, Central Libya. Journal of Volcanology and Geothermal Research, 325, 189-202.

Engelder, T., 1993. Stress regimes in the lithosphere. Princeton University Press, Princeton, New Jersey, U.S.A. 475 pp.

Fatmi, A.N., Eliagoubi, B.A., Hammuda, O.S., 1980. Stratigraphic nomenclature of the pre-Upper Cretaceous Mesozoic rocks of Jabal Nafusah, NW Libya, in: Salem, M.J., Busrewil, M.T. (Eds.), The Geology of Libya. Al-Fatah Université, 2nd Symposium Faculté des Sciences, Tripoli I, 57-66.

Gale, J.F.W., Lander, R.H., Reed, R.M., Laubach, S.E., 2010. Modelling fracture porosity evolution in dolostone. Journal of Structural Geology 32(9), 1201-1211.

Geological Map of Libya at 1:1,000,000 (1985). Compiled by industrial Research Centre, Geological Research and Mining Department, Tripoli, Libya.

Geologic maps of Libya at 1:250,000 of Gebel Qararat-al-Marar (1983) and Gebel Idri (1984), industrial Research Centre, Geological Research and Mining Department, Tripoli, Libya.

Glover, T., Adamson, K., Whittington, R., Fitches, B., Craig, J., 2000. Evidence for soft-sediment deformation; the Duwaysah slide of the Gargaf Arch, central Libya, in: Sola, M.A., Worsley, D. (Eds.), Geological exploration in Murzuq basin. Elsevier, pp. 417-430.

Goudarzi, G.H., 1980. Structure – Libya, in: Salem, M.J., Bursewil, M.T. (Eds.), The Geology of Libya. Academic Press, London II, 879-892.

Gudmundsson, A., 1992. Formation and growth of normal faults at the divergent plate boundary in Iceland. Terra Nova 4, 464-471.

Guiraud, R., 1998. Mesozoic rifting and basin inversion along the northern African Tethyan margin: an overview. Geological Society, London, Special Publication 132, 217-229.

Guiraud, R., Bosworth, W., Thierry, J., Delplanque, A., 2005. Phanerozoic geological evolution of Northern and Central Africa: an overview. Journal of African Earth Sciences 43, 83-143.

Guiraud, R., Bosworth, W., 1997. Senonian basin inversion and rejuvenation of rifting in Africa and Arabia: synthesis and implications to plate-scale tectonics. Tectonophysics 282, 39-82.

Hallett, D., 2002. Petroleum Geology of Libya. Elsevier Science B.V., Amsterdam, 503 p.

Hammuda, O.S., 1980. Geologic factors controlling fluid trapping and anomalous freshwater occurrence in the Tadrart sandstone, Al Hamadah al Hamra area, Ghadamis basin, in: Salem, M.J., Busrewil, M.T. (Eds.), The geology of Libya 2, pp. 501-508.

Havlicek, V., Massa, D., 1973. Brachiopodes de l'Ordovicien supérieur de Libye occidentale implications stratigraphiques régionales. Géobios 6(4), 267-290.

Heine, C., Müller, R.D., Steinberger, B., Torsvik, T.H., 2008. Subsidence in intracontinental basins due to dynamic topography. Physics of the Earth and Planetary Interiors 171, 252–264.

Jerzykiewicz, T., Ghummed, M.A., Tshakreen, S.O., Abugares, M.M., 2003. The Ghadamis-Sirt basin boundary at the time of the Cretaceous/Tertiary transition, in: Salem, M.J., Khaled, M.O. (Eds.), The Geology of Northwest Libya. National Library, Benghazi, Libya 1, 47-62.

Karasek, R.M., 1981. Structural and stratigraphic analysis of the Palaeozoic Murzuq and Ghadames Basins, western Libya. ESRI Occasional Publications, Columbia, S. Carolina. 1, 146p.

Klitzsch, E., 1963. Geology of the northeast flank of the Murzuq Basin, in: South-Central Libya and Northern Chad. A guide book to the geology and prehistory. Petroleum Exploration Society of Libya 19-32.

Klitzsch, E., 1966. Stratigraphic sections from the type areas of Silurian and Devonian strata at Western Murzuq Basin (Libya), in: Kanes, W.H. (Ed.), Archaeology and Prehistory of the south-western Fezzan, Libya. P.E.S.L., 11th Annual Field Conference Guide Book Geology, pp. 83-90.

Klitzsch, E., 1970. Die Strukturgeschichte der Zentralsahara. Neue Erkenntnisse zum Bau und zur Paläogeographie eines Tafellandes. Geologische Rundschau 59, 459-527.

Klitzsch, E., 1981. Lower Palaeozoic rocks of Libya, Egypt and Sudan, in: Holland, C.H. (Ed.), Lower Palaeozoic Rocks of the World 3, 131-163.

Klitzsch, E., 2000. The structural development of the Murzuq and Kufra basins, significance for oil and mineral exploration, in: Sola, M.A., Worsley D. (Eds.), Geological Exploration in Murzuq Basin. Elsevier Science, pp. 143-150.

Kröner, A., 1991. The Pan-African belt of north-eastern and eastern Africa, Madagascar, southern India, Sri Lanka and east Antarctica; Terrane amalgamation during formation of the Gondwana Supercontinent, in: Thorwiehe, U., Schandelmeier, H. (Eds.), Geoscientific research in Northeast Africa. Rotterdam, Netherlands, A.A., Balkema, pp. 3-9.

Laubach, S.E., Olson, J.E., Gross, M.R., 2009. Mechanical and fracture stratigraphy. American Association of Petroleum Geologists Bulletin 93(11), 1413-1426.

Laubach, S.E., Eichhubl, P., Hilgers, C., Lander, R.H., 2010. Structural diagenesis. Journal of Structural Geology 32, 1866-1872.

Lelubre, M., 1946. Sur le Paléozoïque du Fezzan. Comptes Rendus de l'Académie des Sciences de Paris 222, 1403-1404.

Levorsen, A.I., 1954. Geology of Petroleum. W.H. Freeman and Company, San Francisco, 703p.

Massa, D., Delort, T., 1984. Evolution du basin de Syrte (Libye) du Cambrien au Crétacé basal. Bulletin de la Société géologique de France XXVI(6), 1087-1096.

Massa, D., Jaeger, H., 1971. Données stratigraphiques sur le Silurien de l'Ouest de la Libye. Coll. Ordovicien-Silurien, Brest (France), Mémoires du Bureau de Recherches Géologiques et Minières 73, 313-321.

Massa, D., Moreau-Benoit, A., 1976. Essai de synthèse stratigraphique et palynologique du système Dévonien en Libye Occidentale. Revue de l'Institut Français du Pétrole XXXI(2), 287-333.

Montgomery, S., 1994. Petroleum Frontiers. Petroleum Information Corporation, 10 (4), 77 pp.

Moores, E.M., Twiss, R.J., 1992. Stuctural Geology. W.H. Freeman and Company, San Francisco, pp. 40, 62, 200.

Olson, E., Laubach, S.E., Lander, R.H., 2009. Natural fracture characterization in tight gas sandstones: integrating mechanics and diagenesis. American Association of Petroleum Geologists Bulletin 93(11), 1535-1549.

Peña, S.A., Abdelsalam, M.G., 2006. Orbital remote sensing for geological mapping in southern Tunisia: implication for oil and gas exploration. Journal of African Earth Sciences 44, 203–219.

Pollard, D.D., Segal, P., Delaney, P.T., 1982. Formation and interpretation of dilatants echelon cracks. Geological Society of America Bulletin 93, 1291-1303.

Ramsay, J.G., 1987. The techniques of modern structural geology: folds and fractures. Academic Press, 392p.

Rubino, J.-L., Blanpied, C., 2000. Sedimentology and sequence stratigraphy of the Devonian to lowermost Carboniferous succession on the Gargaf Uplift (Murzuq Basin, Libya),

in: Sola, M.A., Worsley, D. (Eds.), Geological Exploration in Murzuq Basin. Elsevier, 321-348.

Said, F.M., 1974. Sedimentary history of the Palaeozoic rocks of the Ghadames Basin, Libyan Arab Republic. Unpubl. M.S. Thesis, University of South Carolina, Columbia, SC.

Said, F.M., Kanes, W.H., 1985. Palaeozoic producing sequences in Ghadamis basin of Libya, Tunisia and Algeria – new stratigraphic concept for hydrocarbon exploration. American Association of Petroleum Geologists Bulletin 69(2), 304.

Scotese, C.R., McKerrow, W.S., 1990. Revised world maps an introduction, in: McKerrow, W.S., Scotese, C.R. (Eds.), Paleozoic Paleogeography and Biostratigraphy. Geological Society of America bulletin 12, 1-21.

Scotese, C.R., Boucot, A.J., McKerrow, W.S., 1999. Gondwana paleogeography and paleoclimatology. Journal of African Earth Sciences 28, 99-114.

Sharp, I.R., Gawthorpe, R.L., Underhill, J.R., Gupta, S., 2000. Fault-propagation folding in extensional settings: examples of structural style and synrift sedimentary response from the Suez rift, Sinai, Egypt. Geological Society of America Bulletin 112(12), 1877–1899.

Sikander, A.H., 2000. Structural development, geology and hydrocarbon potential of the Ghadamis and Murzuq basins – an overview, in: Salem, M.J., Oun, K.M. (Eds.), The Geology of Northwest Libya. National Library, Benghazi, Libya 2, 281-326.

Stampfli, G.M., Borel, G.D., 2002. A plate tectonic model for the Paleozoic and Mesozoic constrained by dynamic plate boundaries and restored synthetic oceanic isochrones. Earth and Planetary Science Letters 196, 17-33.

Laubach, S.E., Jackson, M.L.W., 1990. Origin of arches in Northwestern Gulf of Mexico basin. Geology 18, 595-598.

Sutcliffe, O.E., Dowdeswell, J.A., Whittington, R.J., Theron, J.N., Craig, J., 2000. Calibrating the Late Ordovician glaciation and mass extinction by the eccentricity cycles of Earth's orbit. Geology 28(11), 967-970.

Vos, R.G., 1981. Deltaic sedimentation in the Devonian of Western Libya. Sedimentary Geology 29, 67-88.

Whitbread, T., Kelling, G., 1982. Marar formation of Western Libya, evolution of an early Carboniferous Delta System. American Association of Petroleum Geologists Bulletin 66(8), 1091-1107.

Willis, D.B., 1981. Deposition of the Tadrart Sandstone in the Ghadames Basin, Libya. M. S. Thesis, Univ. South Carolina, U.S.A., 40 p.

Ziegler, P.A., 1988. Geodynamics of Rifting, in: Ziegler, P.A. (Ed.), Case History studies on Rifts: North and South America, Africa–Arabia. Tectonophysics 213, 141–151.

Acknowledgments

We gratefully thank the Libyan Petroleum Institute, Tripoli, Libya for financial, data and fieldwork support. We wish to express our deep thanks and gratitude to GDTA (Groupement pour le Développement de la Télédétection Aérospatiale, in Toulouse, France) and Beicip-Franlab for training of M.B. We have taken profit from Andrea Sharrer, James W. Granath and Gary L. Prost for valuable criticism clarifying our text and figures. We greatly thank William Bosworth and an anonymous reviewer for very helpful review comments.